3-1997

New and Improved Parameters of HD 202908=ADS 14839: A Spectroscopic-Visual Triple System

Francis C. Fekel
Tennessee State University

Colin D. Scarfe
University of Victoria

David J. Barlow
University of Victoria

Antoine Duquennoy
Observatoire de Genève

Harold A. McAlister
Georgia State University

See next page for additional authors

Recommended Citation

Fekel, F.C.; Scarfe, C.D.; Barlow, D.J.; Duquennoy, A.; McAlister, H.A.; Hartkopf, W.I.; Mason, B.D.; Tokovinin, A.A. "New and Improved Parameters of HD 202908=ADS 14839: A Spectroscopic-Visual Triple System" Astronomical Journal v.113, p.1095 (1997)

Authors

Francis C. Fekel, Colin D. Scarfe, David J. Barlow, Antoine Duquennoy, Harold A. McAlister, William I. Hartkopf, Brian D. Mason, and Andrei A. Tokovinin

THE ASTRONOMICAL JOURNAL VOLUME 113, NUMBER 3 MARCH 1997

NEW AND IMPROVED PARAMETERS OF HD 202908=ADS 14839: A SPECTROSCOPIC-VISUAL TRIPLE SYSTEM

FRANCIS C. FEKEL[1]

Department of Physics and Astronomy, Vanderbilt University, Nashville, Tennessee 37235, and Center for Automated Space Science and Center of Excellence in Information Systems, Tennessee State University, 330 Tenth Avenue North, Nashville, Tennessee 37203-3101
Electronic mail: fekel@coe.tnstate.edu

C. D. SCARFE[2] AND D. J. BARLOW

Department of Physics and Astronomy, University of Victoria, Victoria, British Columbia V8W 3P6, Canada
Electronic mail: scarfe@uvphys.phys.uvic.ca, barlow@uvvm.uvic.ca

ANTOINE DUQUENNOY[3]

Observatoire de Genève, 51 chemin des Maillettes, CH-1290 Sauverny, Switzerland

HAROLD A. MCALISTER,[1,4] WILLIAM I. HARTKOPF,[1,4] AND BRIAN D. MASON[1,4]

Center for High Angular Resolution Astronomy, Georgia State University, Atlanta, Georgia 30303-3083
Electronic mail: hal@chara.gsu.edu, hartkopf@chara.gsu.edu, mason@chara.gsu.edu

ANDREI A. TOKOVININ

Sternberg Astronomical Institute, 119899 University Prospect, 13 Moscow, Russia
Electronic mail: toko@sai.msu.su

Received 1996 October 14; revised 1996 November 26

ABSTRACT

HD 202908=ADS 14839 is a spectroscopic-visual triple system consisting of three solar-type stars. Eighteen years of spectroscopic observations including coverage of the recent periastron of 1987 January plus visual and speckle observations, the latter covering roughly the same interval as the radial velocities, have been used to obtain a simultaneous three-dimensional orbital solution. The short-period pair, Aa and Ab, has an orbital period of 3.9660465 days and a small but real eccentricity of 0.0033. The visual pair, A and B, has an orbital period of 78.5 yr and an eccentricity of 0.865. The solution yields masses for all three stars with uncertainties of about 2%, and the distance to the system with an uncertainty of 1.3%. Spectroscopic luminosity ratios, combined with the above distance, yield absolute magnitudes with uncertainties of about 0.1 mag. Thus the system provides three well-determined points on the mass–luminosity relationship. The inclinations of the short- and long-period orbits differ by 29°, making the orbits noncoplanar. Assuming synchronous rotation, the rotational and orbital axes of the short-period pair are aligned. The chromospheric emission, lithium abundance, and projected rotational velocity of component B indicate that the system is quite young, probably about the age of the Hyades Cluster. A comparison with theoretical evolutionary tracks supports such a conclusion. *© 1997 American Astronomical Society.* [S0004-6256(97)01203-X]

1. INTRODUCTION

HD 202908=ADS 14839 AB [$\alpha=21^h\ 18^m\ 34\overset{s}{.}6$, $\delta=11°34'11''$ (2000), $V=7.02$] is a close visual binary, one component of which is also a double-lined spectroscopic binary. It is thus a classic example of a subset of multiple stars called spectroscopic-visual triples. Such systems are of great value since in the best cases fundamental parameters including the mass, luminosity, and spectral type for each component as well as the distance to the system can be obtained. We follow the identification of the components given by Fekel (1981) where component A is the visual primary and consists of a short-period binary whose components are Aa and Ab, while component B is the visual secondary and, thus, the "distant" companion to the short-period system. The C, D, and E components of ADS 14839—magnitudes 13.5, 13, and 11, respectively—are all rather distant from the AB pair and are excluded from the discussion.

[1]Visiting Astronomer, Kitt Peak National Observatory, National Optical Astronomy Observatories, operated by the Association of Universities for Research in Astronomy, Inc., under contract with the National Science Foundation.
[2]Visiting Astronomer, Dominion Astrophysical Observatory, National Research Council of Canada.
[3]Deceased.
[4]Visiting Astronomer, Mount Wilson Observatory, operated under a collaborative agreement between the Carnegie Institution of Washington and the Mount Wilson Institute.

More than 120 years ago Burnham (1873) launched HD 202908 into a state of limited astronomical notoriety with his discovery that this star is a close visual binary, later designated Bu 163 AB. Additional visual observations over the next 50 years revealed that the system has a high inclination and large eccentricity, and a preliminary visual orbit eventually was computed (Aitken 1932). A more recent orbit by Heintz (1969) predicted that the next periastron passage would occur at 1985.5. Visual observations continued unabated until the early 1980s when such measurements became increasingly difficult as the visual pair approached periastron. Fortunately, speckle-interferometric observations, able to resolve the pair at closer separations, were begun in the mid 1970s and have continued to the present [see Hartkopf *et al.* (1995) for a summary]. Using observations through periastron, Heintz (1994) revised his earlier orbit. The latest orbit has a period of 77.4 yr, a rather large eccentricity of 0.865, an inclination of 98°8, and a revised time of periastron passage of 1987.18.

In the 1940s HD 202908 was placed on the spectroscopic-survey program at Mt. Wilson, resulting in the next major advance in our knowledge of the system. From 12 moderate or high-dispersion plates Wilson (Wilson & Joy 1950) found component A to be a double-lined spectroscopic binary and obtained a preliminary period of 3.97 days and a mass ratio of unity for the short-period pair, Aa and Ab.

Nearly twenty years later, the system was included as part of several survey programs of spectral classification and photometry. Spectral classification of the system as a whole indicates a spectral type slightly earlier than solar (Christy & Walker 1969; Harlan 1969; Abt 1981). The Strömgren $b-y$ index of Perry (1969) and Johnson colors of Barnes and Moffett (Fekel 1981) are consistent with this classification.

It was not until the mid 1970s that significant additional spectroscopic observations were obtained. Fekel (1981) reported the results of high-dispersion spectroscopic observations that showed absorption features of all three stars. He revised the orbital period of Wilson & Joy (1950) to 3.9660 days, confirmed that the mass ratio of the pair is very close to unity, and showed that the individual components have similar spectral types. That orbit was inadvertently left out of the latest catalog of spectroscopic orbits (Batten *et al.* 1989). Recently, Fekel (1992) computed a preliminary long-period spectroscopic orbit for component B. Comparison of the inclinations of the short- and long-period orbits (Fekel 1981) indicated that the system is noncoplanar.

Fekel (1981) found that all three stars have Ca II K line emission. As a result, HD 202908 is listed in *A Catalog of Chromospherically Active Binary Stars* (Strassmeier *et al.* 1993). Henry *et al.* (1995) searched for possible associated light variations but found none.

During the last two decades this system was placed on the observing programs of other astronomers at observatories around the world. Communication between us has resulted in the present collaboration to determine the fundamental parameters of this system.

2. RADIAL VELOCITY OBSERVATIONS AND REDUCTIONS

Since 1975 extensive sets of radial-velocity observations have been obtained at several observatories. Most of those data are presented here for the first time.

From 1975 through 1977, 15 photographic spectrograms were obtained by F.C.F. at blue wavelengths with the McDonald Observatory's 2 m telescope and coudé spectrograph. A description of the plates and the velocity-measurement procedure was given by Fekel (1981). A correction of -0.5 km s^{-1} has been added to the measured plate velocities to place them on the velocity system of Scarfe *et al.* (1990).

F.C.F. also obtained 14 observations from 1976 through 1981 with the McDonald Observatory's 2.7 m telescope, coudé spectrograph, and a Reticon RL-1024B self-scanned silicon photodiode array. Most of those observations had a resolution of 0.33 Å and were centered at 6430 Å but a couple were obtained of the lithium region at 6700 Å. Details of the velocity-reduction procedure have been given by Fekel *et al.* (1978). The velocities were measured relative to o Aql (HR 7560) or ι Psc, two IAU radial-velocity standards (Pearce 1957), whose velocities have been adopted from the work of Scarfe *et al.* (1990). Both the photographic and Reticon velocities that appear in Table 1 have slightly different values from those listed by Fekel (1981).

From 1982 through 1994, F.C.F. obtained 61 observations of HD 202908 (Table 1) at the Kitt Peak National Observatory (KPNO) with the coudé feed telescope, coudé spectrograph, and various charge-coupled devices (CCDs). While two observations were obtained in 1982 with a Fairchild CCD and two in 1983 with an RCA CCD, all the rest were obtained with a Texas Instruments (TI) CCD. Parameters for the Fairchild and RCA CCD observations are given by Fekel (1991). Observations with the TI detector cover a wavelength range of about 80 Å and have a resolution of 0.21 Å. One of the CCD observations was centered at 6695 Å to include the lithium line at 6708 Å, while all the rest have been centered at 6430 Å. Most of the spectra, one of which is shown in Fig. 1, have signal-to-noise ratios of 150:1 or better. Like the Reticon spectra each KPNO CCD spectrum was measured relative to either o Aql or ι Psc with the velocity-reduction procedure of Fekel *et al.* (1978).

In 1977 a series of observations of HD 202908 was begun with the CORAVEL radial-velocity spectrometer on the 1 m Swiss telescope at Haute-Provence Observatory. The observations were made by several different observers. Radial velocities were determined by A.D. with the methods discussed by Duquennoy (1987) for the measurement of unblended and blended cross-correlation dips. These radial velocities are given in Table 2.

Another series of observations of HD 202908 has been obtained by C.D.S. with the Dominion Astrophysical Observatory (DAO) radial-velocity spectrometer, in both its original (Fletcher *et al.* 1982) and current (McClure *et al.* 1985) configurations. Observations were begun early in 1981 and have continued to the present. Masks based on the spectra of Procyon and Arcturus have been found to give about equally good results, and all those available have been used at one

TABLE 1. McDonald and Kitt Peak radial velocities.

Hel. J.D. −2440000	Instrument code	Light-time correction (days)	Long-period phase	Short-period phase	V_{Aa} km s^{-1}	O-C$_{Aa}$ km s^{-1}	V_{Ab} km s^{-1}	O-C$_{Ab}$ km s^{-1}	V_B km s^{-1}	O-C$_B$ km s^{-1}
2706.769	MP	-0.016	0.857	0.542	-58.6	-0.4	74.0	0.9	6.9	-0.7
2708.731	MP	-0.016	0.857	0.036	69.6	-0.3	-60.2	1.9	4.6	-3.0
2712.745	MP	-0.016	0.857	0.049	68.5	0.0	-58.9	1.8	6.5	-1.1
2882.985	MP	-0.016	0.863	0.973	71.4	0.6	-61.2	1.9	7.1	-0.4
2884.972	MP	-0.016	0.863	0.474	-61.9	-2.5	76.4	2.1	7.2	-0.3
2997.920	MP	-0.017	0.867	0.953	65.8	-3.2	-59.8	1.3	5.6	-1.9
2999.841	MP	-0.017	0.867	0.437	-56.3	-1.2	70.1	0.3	7.4	-0.1
3001.902	MP	-0.017	0.867	0.957	69.0	-0.4	-61.3	0.3	6.4	-1.1
3061.735	MP	-0.017	0.869	0.043	69.8	0.6	-60.1	1.2	5.4	-2.1
3063.682	MP	-0.017	0.869	0.534	-58.0	0.9	72.9	-1.0	6.4	-1.1
3085.630	MP	-0.017	0.870	0.068	65.5	-0.1	-56.0	1.5	4.5	-3.0
3087.657	MP	-0.017	0.870	0.579	-53.8	-1.3	66.2	-0.9	6.6	-0.9
3088.595	MR	-0.017	0.870	0.816	31.3	-1.0	-19.9	2.5	8.0	0.5
3089.576	MR	-0.017	0.870	0.063	67.2	0.7	-56.4	2.0	7.7	0.2
3090.646	MR	-0.017	0.870	0.333	-27.0	-0.1	39.7	-0.4	6.9	-0.6
3121.560	MP	-0.017	0.871	0.127	49.9	-1.6	-44.4	-1.8	5.7	-1.8
3269.922	MP	-0.017	0.876	0.536	-59.3	-0.6	74.0	0.2	5.5	-1.9
3390.892	MP	-0.017	0.881	0.037	70.4	0.5	-59.3	2.6	6.5	-0.8
3445.649	MR	-0.017	0.883	0.843	42.1	-0.5	-31.6	1.5	7.7	0.4
3448.584	MR	-0.017	0.883	0.584	-50.9	0.7	68.1	1.8	7.6	0.3
3741.841	MR	-0.018	0.893	0.526	-59.6	-0.2	75.2	0.5	7.8	0.7
4178.713	MR	-0.018	0.908	0.679	-22.4	0.4	36.7	0.3	7.5	0.7
4179.631	MR	-0.018	0.908	0.910	61.4	-0.6	-53.3	-0.2	6.5	-0.3
4357.988	MR	-0.018	0.914	0.881	53.8	-1.0	-43.9	1.4	5.4	-1.2
4475.770	MR	-0.018	0.918	0.579	-53.0	-0.8	67.4	-0.2	6.1	-0.4
4736.977	MR	-0.018	0.928	0.440	-54.5	0.4	71.0	0.2	5.9	-0.3
4832.888	MR	-0.018	0.931	0.623	-40.3	1.0	55.1	-1.5	7.1	1.1
4895.581	MR	-0.018	0.933	0.430	-53.2	0.0	69.9	0.7	5.7	-0.2
4897.702	MR	-0.018	0.933	0.965	70.8	-0.1	-61.9	-0.2	6.1	0.2
5077.999	KF	-0.018	0.939	0.425	-52.2	-0.1	67.0	-1.4	5.8	0.2
5080.002	KF	-0.018	0.940	0.930	65.1	-1.3	-55.7	1.0	5.5	-0.1
5449.001	KR	-0.018	0.952	0.969	70.9	-0.9	-56.7	4.9*	6.0	1.3
5450.979	KR	-0.018	0.952	0.468	-59.1	-1.4	74.2	-0.9	5.3	0.6
5525.895	KT	-0.018	0.955	0.357	-34.4	-0.4	49.8	-0.5	4.1	-0.3
5527.931	KT	-0.018	0.955	0.871	52.7	0.0	-41.1	0.0	4.5	0.1
5595.732	KT	-0.017	0.958	0.966	72.4	0.6	-60.0	1.1	4.8	0.6
5814.006	KT	-0.017	0.965	0.001	74.1	0.5	-61.9	0.2	3.3	0.2
5851.984	KT	-0.016	0.966	0.577	-51.1	-0.2	69.2	-0.3	2.0	-0.9
5853.944	KT	-0.016	0.967	0.071	66.5	-0.5	-55.6	-0.7	1.8	-1.1
5942.752	KT	-0.016	0.970	0.463	-56.4	-0.2	76.0	0.3	2.6	0.3
5972.784	KT	-0.016	0.971	0.036	71.5	-0.9	-60.0	-0.2	1.4	-0.7
5974.774	KT	-0.016	0.971	0.537	-55.4	0.9	75.6	-0.4	2.4	0.3
6389.664	KT	-0.012	0.985	0.147	50.1	-0.1	-30.6	0.7	-3.5	0.1
6390.680	KT	-0.012	0.985	0.403	-43.1	0.3	67.5	0.0	-3.8	-0.2
6392.688	KT	-0.012	0.985	0.909	66.9	0.5	-47.8	0.5	-3.7	0.0
6531.986	KT	-0.009	0.990	0.031	76.0	-1.1	-56.4	-0.6	-7.5	0.4
6534.001	KT	-0.009	0.990	0.539	-50.4	1.3	80.6	0.5	-7.7	0.3
6583.854	KT	-0.008	0.992	0.109	65.2	0.9	-40.7	-0.3	-9.2	0.8
6586.979	KT	-0.008	0.992	0.897	66.1	-0.2	-42.0	0.4	-10.5	-0.4
6718.586	KT	-0.004	0.997	0.079	73.9	-0.1	-43.9	0.9	-16.3	0.2
6867.043	KT	0.001	0.002	0.510	-48.6	-0.2	86.9	-0.2	-19.4	0.1
6869.038	KT	0.001	0.002	0.013	83.8	0.5	-51.7	0.2	-20.6	-1.2
6963.939	KT	0.005	0.005	0.941	77.3	-0.6	-47.9	0.9	-16.8	-0.2
6973.950	KT	0.005	0.006	0.465	-47.8	0.4	83.0	-1.0	-15.6	0.6
7096.689	KT	0.009	0.010	0.411	-40.7	1.1	72.6	-0.3	-11.8	-0.2
7098.716	KT	0.009	0.010	0.922	72.5	0.0	-48.1	-0.4	-11.7	-0.2
7150.599	KT	0.010	0.012	0.004	79.3	0.0	-56.2	0.2	-9.8	0.0
7152.597	KT	0.010	0.012	0.507	-52.8	-0.1	83.2	0.3	-10.5	-0.7
7246.025	KT	0.012	0.015	0.064	72.3	-0.5	-51.3	0.5	-8.9	-1.6
7308.986	KT	0.013	0.017	0.939	73.4	0.5	-53.7	-0.6	-5.6	0.4
7310.980	KT	0.013	0.017	0.441	-50.0	-0.1	76.2	-0.2	-5.6	0.3
7312.983	KT	0.013	0.017	0.946	73.9	-0.1	-54.4	0.0	-6.1	-0.2
7453.732	KT	0.015	0.022	0.434	-50.3	-0.5	73.8	-0.4	-4.6	-1.0
7457.765	KT	0.016	0.022	0.451	-52.0	0.3	77.6	0.8	-3.9	-0.3
7624.988	KT	0.018	0.028	0.614	-40.5	-0.3	62.5	0.1	-2.6	-0.9
7627.012	KT	0.018	0.028	0.125	56.1	-0.2	-39.6	-0.1	-2.4	-0.7
7810.759	KT	0.020	0.035	0.454	-54.0	0.1	75.8	0.1	-0.3	-0.1
7812.769	KT	0.020	0.035	0.961	72.2	-1.0	-59.2	-0.5	-0.5	-0.3
7814.683	KT	0.020	0.035	0.444	-52.2	0.5	74.0	-0.2	0.2	0.4
8060.919	KT	0.022	0.044	0.529	-56.4	0.2	77.0	-0.1	1.4	0.2
8163.747	KT	0.022	0.047	0.456	-55.4	-0.2	74.4	-0.8	0.8	-0.9
8167.703	KT	0.022	0.047	0.453	-54.7	0.2	74.6	-0.2	1.6	-0.1
8346.017	KT	0.024	0.053	0.413	-48.2	0.1	67.1	-0.2	2.2	-0.1
8425.878	KT	0.024	0.056	0.549	-54.9	0.3	74.3	0.0	2.7	0.1
8506.736	KT	0.024	0.059	0.937	68.7	-0.1	-56.2	0.5	3.2	0.4
8508.692	KT	0.024	0.059	0.430	-51.3	0.5	70.7	0.1	2.4	-0.4
8572.619	KT	0.025	0.061	0.548	-53.2	2.3*	74.8	0.5	1.7	-1.3
8578.554	KT	0.025	0.062	0.045	71.1	0.1	-59.0	0.2	3.0	0.0
8604.576	KT	0.025	0.062	0.606	-44.6	-0.1	62.7	0.1	2.9	-0.2
8770.946	KT	0.026	0.068	0.554	-55.2	-0.3	73.4	0.1	3.3	-0.2
8913.779	KT	0.026	0.073	0.568	-52.5	0.4	70.6	-0.3	3.2	-0.6
8915.747	KT	0.026	0.073	0.064	68.6	0.7	-57.0	-0.4	3.6	-0.2
9101.991	KT	0.027	0.080	0.024	72.6	0.2	-61.6	0.1	4.2	0.1
9246.655	KT	0.027	0.085	0.499	-59.1	-0.1	77.2	0.4	3.7	-0.6
9248.690	KT	0.027	0.085	0.013	73.8	0.9	-62.5	-0.1	4.3	0.0
9302.573	KT	0.027	0.087	0.599	-46.9	0.0	64.7	0.7	4.7	0.3
9458.981	KT	0.028	0.092	0.035	71.7	0.4	-61.6	-0.7	4.5	-0.1
9465.002	KT	0.028	0.092	0.553	-54.6	1.0	72.5	-0.4	4.8	0.2
9619.650	KT	0.028	0.098	0.546	-55.4	1.1	73.9	0.2	5.4	0.6
9621.636	KT	0.028	0.098	0.047	70.1	0.2	-58.9	0.8	4.3	-0.5

Notes to TABLE 1

1. An asterisk beside a residual implicates that the residual is larger than three times the root-mean-square value for observations of the same weight as the one indicated; such observations were rejected from the final orbital solution.

2. Instrument codes: MP—McDonald Photographic, MR—McDonald Reticon, KF—Kitt Peak Fairchild CCD, KR—Kitt Peak RCA CCD, KTK—Kitt Peak Texas Instruments CCD.

time or another. Observations of IAU standard stars (Pearce 1957) have been used to adjust the observations made with each mask to the zero-point of Scarfe *et al.* (1990). Those adjustments are given in a footnote to Table 3.

The DAO velocities are set out in Table 3. It was not found necessary to apply corrections for blending, of the kind described by Scarfe *et al.* (1991), but a few velocities obtained from blended profiles have been rejected and omitted from that table. The total number of usable velocities from DAO radial-velocity scanner observations is 86 of each component of the close pair and 81 of the fainter distant companion, after rejection of those velocities that yielded residuals over three times the root-mean-square value for the DAO velocities of the relevant star.

The last large set of radial-velocity observations was obtained by A.A.T. from 1986 through 1992, at the Crimean Astrophysical Observatory and Simeis Observatory, with three different telescopes ranging from 0.6 to 1.25 m and a correlation radial-velocity meter similar to CORAVEL (Tokovinin 1987). The process of data reduction was somewhat different from the standard one since the lines were frequently blended. Hence the width and depth of the correlation dip of each component were first determined from good records obtained without line blending. Then the blended observations were reduced with the width and sometimes contrast of the lines kept at fixed values previously determined so as to disentangle the individual velocities of the components. In this data set (Table 4) there are 27 velocities of Aa, 24 of Ab, and 14 of B.

3. VISUAL AND SPECKLE OBSERVATIONS

As stated above, Bu 163 AB has been followed by visual observers for well over a century. The database of the Washington Double Star Catalogue, maintained by Charles Worley of the U.S. Naval Observatory (e.g., Worley 1992), includes 126 measures of this system to date; the 122 measures with complete separation and position-angle information are listed in Table 5. Following the usual convention of visual observers, dates in this table are given in fractional Besselian years; additional information includes orbital phase (based on the orbital elements derived below), published position angle and residual (in degrees), and separation angle and residual (in arcseconds). The final two columns give each measure's relative weight in the orbital solution and a code for the aperture of the telescope used: "S" for a "small" telescope (aperture <0.45 m) or "L" for a "large" telescope. Hartkopf *et al.* (1989) discussed the role of aperture size and other factors in determining relative weights of visual and interferometric measures.

Speckle interferometric observation of this system began in 1977 (McAlister & Hendry 1982); 36 measures (plus one unresolved observation) are listed in Hartkopf *et al.* (1995). These measures, as well as six others previously unpublished, are given in Table 6. Here the first six columns are the same as in Table 5: the final three columns give the telescope aperture in meters, the relative weight of the measure, and a code for the original reference.

The first "new" measure resulted from data obtained at the KPNO 3.8 m Mayall telescope in 1988 with the CHARA speckle equipment and an intensified RCA CCD camera (McAlister *et al.* 1987). The pair was only marginally resolved at this epoch, and the resulting measure was originally considered too uncertain for publication. These data were recently reanalysed with the use of the "directed vector autocorrelation" technique described by Bagnuolo *et al.* (1992); this resulted in an improved measure, although still not good enough to avoid being rejected in the final orbital solution.

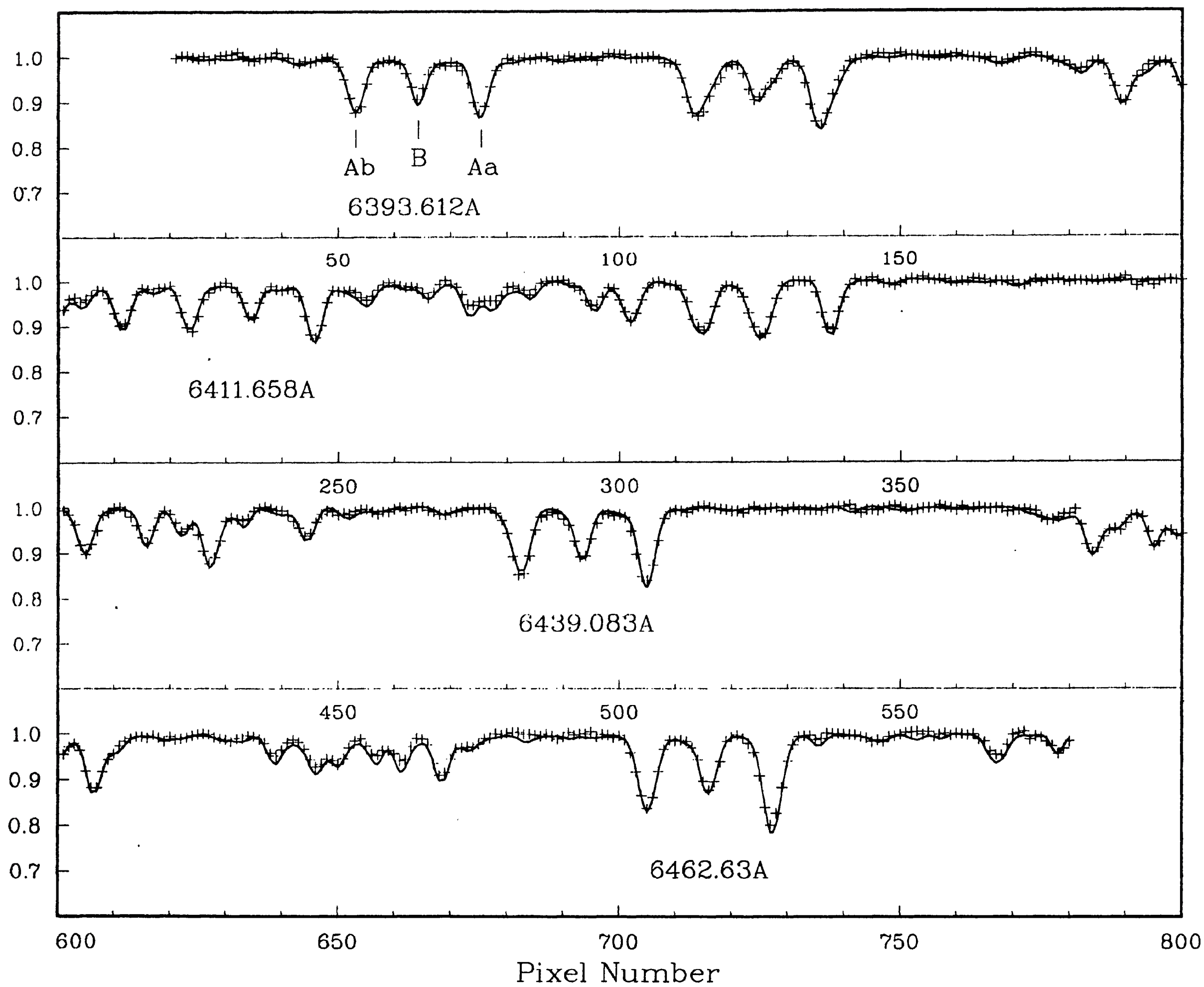

FIG. 1. A red-wavelength spectrum of HD 202908 in the 6430 Å region is shown as pluses. Superposed as a continuous curve are weighted spectra of HR 7560 for Aa, HR 7560 for Ab, and HR 483 for B. The vertical axis is relative intensity. The rest wavelengths of several lines are identified.

The remaining new measures were obtained with the same speckle equipment and an ITT ICCD speckle camera (Mason *et al.* 1993). Data for four of these were obtained at the Mt. Wilson 2.5 m telescope, following the renovation and reopening of this historic instrument in 1993 November, while data for the 1994 measure were obtained at the KPNO 3.8 m telescope.

4. ORBITAL SOLUTIONS

Differential-correction programs to determine the spectroscopic, visual, and three-dimensional (simultaneous spectroscopic-visual) orbits for binary or triple systems, based on the method of nonlinear least squares, have been developed at the University of Victoria (by D.J.B.), and used in recent studies of Capella (Barlow *et al.* 1993) and HR 6469 (Scarfe *et al.* 1994). The triple-system programs include all the elements of both orbits (circular or elliptical), permit the use of light-time corrections, and can handle any combination of one, two or three measurable spectra. Orbits of small eccentricity use Sterne's (1941) equation of condition, in which T_0 is used in place of T. The sum of the weighted squares of residuals is minimized in preliminary individual solutions of the position angles θ_i, separations ρ_j, and radial velocities V_k, and the quantity

$$\sum_i w_i(\Delta\theta_i/\sigma_\theta)^2+\sum_j w_j(\Delta\rho_j/\sigma_\rho)^2+\sum_k w_k(\Delta V_k/\sigma_V)^2$$

is minimized for the three-dimensional solutions (the first two terms only for visual binaries without radial-velocity data). In this expression, σ_θ, σ_ρ, and σ_V are the standard errors of an observation of unit weight obtained from the individual solutions, respectively. All solutions that use data of more than one kind yield new values of the appropriate σ's; these should not differ significantly from their input values if the data are mutually compatible. We have used these programs to obtain several solutions for the orbital elements of HD 202908, which are described in the next few paragraphs.

First, the visual and speckle data set out in Tables 5 and 6, respectively, were used to obtain solutions for the "visual" elements. We adopted the weighting system of Hartkopf *et al.* (1989), in which the CHARA speckle data were as-

TABLE 2. CORAVEL radial velocities.

Hel. J.D. −2440000	Light-time correction (days)	Long-period phase	Short-period phase	V_{Aa} km s^{-1}	O-C$_{Aa}$ km s^{-1}	V_{Ab} km s^{-1}	O-C$_{Ab}$ km s^{-1}	V_B km s^{-1}	O-C$_B$ km s^{-1}
3379.448	-0.017	0.880	0.152	39.6	-4.3*	-29.4	5.0*	--	--
3380.460	-0.017	0.880	0.407	-51.7^{2}	-2.7	65.8^{2}	2.2	8.7	1.4
3388.385	-0.017	0.881	0.405	-50.3	-1.7	66.8	3.6	10.8	3.5
3389.406	-0.017	0.881	0.662	-25.9^{2}	3.1*	37.8^{2}	-4.6*	--	--
3390.414	-0.017	0.881	0.917	65.1^{2}	2.0	-58.3^{2}	-3.5*	--	--
3396.395	-0.017	0.881	0.424	-54.3^{3}	-1.5	70.2^{2}	2.6	--	--
3398.382	-0.017	0.881	0.926	64.6^{2}	-0.3	-61.2^{2}	-4.6*	7.1^{3}	-0.2
3399.318	-0.017	0.881	0.162	37.9	-2.5	--	--	10.5	3.2
3403.417	-0.017	0.881	0.195	22.9^{3}	-5.1*	--	--	3.9^{2}	-3.4*
3434.385	-0.017	0.882	0.004	72.2	0.4	-65.3	-1.4	6.2	-1.1
3447.351	-0.017	0.883	0.273	-3.6^{3}	-0.1	14.2^{3}	-1.4	9.9^{3}	2.6
3451.302	-0.017	0.883	0.269	1.0	3.0	12.7	-1.3	8.8	1.5
3456.271	-0.017	0.883	0.522	-59.3^{3}	0.4	73.4^{3}	-1.5	--	--
3457.314	-0.017	0.883	0.785	20.7^{3}	0.5	-9.2^{3}	0.2	7.0^{3}	-0.3
3458.269	-0.017	0.883	0.025	71.4^{3}	0.5	-64.2^{3}	-1.2	7.4^{3}	0.1
3459.258	-0.017	0.883	0.275	-4.8^{3}	-0.4	18.1^{3}	1.6	6.8^{3}	-0.5
3466.287	-0.017	0.883	0.047	67.4^{3}	-1.4	-60.5^{3}	0.2	6.7^{4}	-0.6
3467.266	-0.017	0.883	0.294	-13.1^{4}	-1.0	24.0^{4}	-0.7	4.3^{4}	-3.0*
3470.260	-0.017	0.883	0.049	68.5^{4}	-0.1	-60.9^{3}	-0.4	--	--
3475.280	-0.017	0.884	0.315	-18.7	1.5	33.1^{3}	-0.1	--	--
3682.529	-0.018	0.891	0.571	-56.2	-2.2	69.1	0.1	7.1	-0.1
3685.583	-0.018	0.891	0.341	-29.1	0.5	41.6	-1.6	8.5	1.3
3686.593	-0.018	0.891	0.595	-49.1	-0.2	64.3	0.7	6.4	-0.8
3696.585	-0.018	0.891	0.115	54.9	-0.3	-47.6	-1.3	7.4	0.2
3697.590	-0.018	0.891	0.368	-37.9	0.7	54.6	1.9	5.7	-1.5
3698.561	-0.018	0.891	0.613	-46.6	-2.1	58.8	-0.1	7.8	0.6
3699.585	-0.018	0.891	0.871	50.1	-1.5	-42.4	0.1	8.0	0.8
3700.588	-0.018	0.891	0.124	51.8	-0.8	-44.1	-0.6	6.1	-1.1
3703.570	-0.018	0.892	0.876	53.5	0.4	-44.1	-0.1	7.1	0.0
3705.578	-0.018	0.892	0.382	-44.4	-1.7	56.2	-0.9	8.0	0.9
3706.566	-0.018	0.892	0.631	-39.9	-0.7	52.9	-0.5	8.7	1.6
3708.587	-0.018	0.892	0.141	46.1	-1.3	-37.9	0.2	1.8	-5.3*
3709.577	-0.018	0.892	0.390	-46.0	-1.1	60.1	0.7	7.3	0.2
3710.546	-0.018	0.892	0.635	-36.0	2.1	53.4	1.2	5.8	-1.3
3711.538	-0.018	0.892	0.885	57.3	1.7	-45.5	1.2	11.1	4.0*
3712.561	-0.018	0.892	0.143	46.7	-0.1	-38.3	-1.0	7.3	0.2
3732.521	-0.018	0.893	0.176	35.3^{2}	-0.2	-25.6^{2}	-0.2	6.5	-0.6
3764.524	-0.018	0.894	0.245	9.4	1.4	4.5	0.9	4.9	-2.2
5910.537	-0.016	0.969	0.341	-27.2^{3}	0.4	44.8^{2}	-0.4	3.1^{2}	0.6
5913.585	-0.016	0.969	0.109	59.1^{2}	0.3	-46.4^{2}	-0.6	2.4	-0.1
5914.528	-0.016	0.969	0.347	-30.3	-0.6	47.7	0.2	1.1	-1.4
5915.529	-0.016	0.969	0.599	-46.3^{2}	-0.4	64.4^{2}	-0.2	2.6^{2}	0.1
5918.467	-0.016	0.969	0.340	-28.0^{2}	-0.7	44.9^{2}	-0.2	2.2^{2}	-0.3
5919.473	-0.016	0.969	0.594	-48.1	-0.9	66.2	0.2	3.4^{2}	0.9
5920.486	-0.016	0.969	0.849	46.8^{2}	0.1	-32.7	0.3	1.5^{2}	-1.0
5929.523	-0.016	0.969	0.128	53.9	0.3	-39.4	0.9	2.8^{2}	0.4
5932.578	-0.016	0.969	0.898	61.3	0.2	-49.2	-1.0	1.9^{2}	-0.5
5933.445	-0.016	0.969	0.117	57.4	0.6	-44.5	-0.9	3.3^{2}	0.9
5942.460	-0.016	0.970	0.390	-42.4	0.3	61.2	-0.2	4.1	1.8
5969.386	-0.016	0.971	0.179	37.3^{2}	0.9	-21.1	0.8	4.7	2.6
6029.341	-0.015	0.973	0.296	-10.3	0.0	30.0	2.1	7.1	5.5*
6127.708	-0.015	0.976	0.098	64.1^{2}	1.6	-49.1^{2}	-1.1	2.9^{2}	2.3
6219.575	-0.014	0.979	0.261	5.3^{2}	0.7	12.7^{2}	-1.4	-3.5^{2}	-3.0
6220.590	-0.014	0.979	0.517	-56.9^{2}	-0.4	79.2	0.7	0.9^{2}	1.4
6223.569	-0.014	0.979	0.268	2.1	0.3	16.4	-0.7	-3.4	-2.8
6246.594	-0.013	0.980	0.073	68.4^{2}	0.1	-53.6^{2}	-0.8	-1.1^{2}	-0.2
6248.524	-0.013	0.980	0.560	-52.7^{2}	-0.5	74.5	0.2	-0.8^{2}	0.1
6249.528	-0.013	0.980	0.813	34.6^{2}	-0.6	-18.1^{2}	-0.3	-1.1^{2}	-0.2
6251.526	-0.013	0.980	0.317	-14.8^{2}	2.7	36.5	-1.2	-1.2	-0.2
6252.497	-0.013	0.980	0.562	-53.1^{2}	-1.3	72.9	-1.1	-1.4^{2}	-0.4
6253.544	-0.013	0.980	0.826	40.9^{2}	1.0	-26.4	-3.7	-6.2	-5.2*
6254.511	-0.013	0.980	0.070	69.3	0.2	-54.0	-0.5	-2.7	-1.7
6255.498	-0.013	0.981	0.319	-15.8^{2}	2.2	38.4	0.0	1.1	2.1
6256.535	-0.013	0.981	0.580	-49.6^{2}	-1.0	70.5	-0.2	-1.8	-0.7
6257.546	-0.013	0.981	0.835	42.7	-0.5	-26.1	0.1	-3.4	-2.3
6277.532	-0.013	0.981	0.874	56.7	0.4	-39.6	0.1	-2.1^{2}	-0.7
6278.547	-0.013	0.981	0.130	53.9^{2}	-0.6	-37.5	0.3	-1.8^{2}	-0.4
6279.529	-0.013	0.981	0.378	-39.0	-1.3	58.3	-1.2	-1.1	0.3
6310.413	-0.013	0.982	0.165	42.8	-0.5	-24.7	0.8	-1.5	0.5
6330.404	-0.013	0.983	0.205	28.5	0.3	-10.4	-1.2	-2.3	0.0
6372.309	-0.012	0.985	0.771	19.0	-0.1	1.5	0.3	-3.6	-0.4
6373.361	-0.012	0.985	0.036	75.0	0.3	-56.9	0.5	-3.0^{2}	0.2
6377.314	-0.012	0.985	0.033	75.8	0.8	-57.3	0.4	-3.1^{2}	0.2
6380.280	-0.012	0.985	0.781	23.1	-0.1	-3.1	-0.1	-4.5	-1.1
6383.319	-0.012	0.985	0.547	-54.0	-1.2	77.5	0.2	-1.6	1.9
6412.258	-0.011	0.986	0.844	48.7	1.0	-25.1	3.0	-3.5	0.7
6419.235	-0.011	0.986	0.603	-41.7	0.4	67.9	1.2	-3.2	1.1
6437.255	-0.011	0.987	0.146	52.4	1.4	-27.6	3.4	-3.6	1.2
6584.605	-0.008	0.992	0.298	-5.9	0.4	34.8	0.7	-11.8	-1.8
6585.604	-0.008	0.992	0.550	-50.0	-0.5	--	--	-11.0	-0.9
6587.619	-0.008	0.992	0.058	--	--	-51.9	-0.4	-9.1	1.1
6619.587	-0.007	0.993	0.119	63.6	1.2	-38.7	-1.8	-13.4	-1.8
6636.523	-0.007	0.994	0.389	-35.5	0.4	67.2	-0.4	-12.2	0.3
6638.459	-0.007	0.994	0.877	61.6	-0.4	-34.7	0.9	-12.6	0.0
6639.518	-0.007	0.994	0.144	55.6	0.4	-27.9	0.5	-14.1	-1.5
6644.523	-0.007	0.994	0.406	-40.7	-0.7	--	--	-13.5	-0.6
6645.577	-0.007	0.994	0.672	-17.1	-0.3	49.2^{2}	1.4	-12.6	0.3
6646.481	-0.007	0.994	0.899	--	--	-42.3	-0.5	-12.7	0.3
6706.342	-0.005	0.996	0.992	82.1	0.1	-53.2	0.5	-17.0	-1.1
6707.369	-0.005	0.996	0.251	14.9	-0.6	16.6	0.1	-17.9	-1.9
6708.347	-0.005	0.996	0.498	-49.9	0.1	--	--	-16.3	-0.3
6746.259	-0.003	0.998	0.057	78.4	-0.1	--	--	--	--
6753.376	-0.003	0.998	0.851	--	--	-25.2	-0.5	-18.9	-0.9
6758.257	-0.003	0.998	0.082	73.3	-1.0	--	--	--	--
6766.251	-0.003	0.998	0.097	70.3	-0.6	-39.8	-0.1	-19.2	-0.7
6767.236	-0.003	0.998	0.346	-20.1	0.0	56.5	0.2	-17.4	1.1
6768.235	-0.003	0.998	0.598	-36.8	0.3	75.0	0.7	-17.8	0.7
6878.680	0.002	0.002	0.444	-42.6	1.8	82.9	0.2	--	--
6883.674	0.002	0.002	0.703	0.5	2.4	37.4	-0.3	-16.2	3.0
6886.678	0.002	0.003	0.461	-46.9	-0.4	--	--	-21.6	-2.5
7029.470	0.007	0.008	0.463	-49.6	-0.6	82.8	0.0	-13.0	1.0
7032.472	0.007	0.008	0.220	25.9	-1.5	0.4	-1.7	-16.0	-2.1
7033.441	0.007	0.008	0.464	-49.5	-0.3	82.3	-0.6	-13.5	0.4
7350.598	0.014	0.019	0.430	-48.4	0.0	75.1	0.9	-5.5	-0.3
7351.556	0.014	0.019	0.672	-20.5	-0.5	44.5	0.3	-4.7	0.5
7352.560	0.014	0.019	0.925	69.8	-0.5	-51.2	-0.1	-5.1	0.1
7353.560	0.014	0.019	0.177	39.0	-1.2	-18.8	0.5	-5.8	-0.7
7364.550	0.014	0.019	0.948	73.6	-0.3	-55.7	-0.7	-3.1	1.9
7368.557	0.014	0.019	0.959	74.4	-0.7	-56.8^{2}	-0.4	-3.8^{2}	1.1
7369.563	0.014	0.019	0.212	26.2^{6}	-0.3	-5.4^{6}	-0.2	-5.0^{6}	-0.1
7370.484	0.014	0.019	0.444	-51.6^{4}	-0.8	74.4^{2}	-2.0	-3.0^{2}	1.9
7371.538	0.014	0.019	0.710	-7.0^{5}	-1.7	28.2^{5}	-0.3	-4.9^{8}	-0.1
7371.577	0.014	0.019	0.720	-1.5	-0.2	24.8	0.6	--	--
7371.622	0.014	0.019	0.731	3.5^{2}	0.2	19.3^{2}	0.0	--	--
7385.490	0.014	0.020	0.228	19.3	-0.7	2.5	1.0	-6.6	-2.0
7397.482	0.015	0.020	0.252	11.9	1.7	9.7	-1.9	-5.3	-0.9
7430.405	0.015	0.022	0.553	-52.7	-0.8	76.3	-0.4	-3.9^{2}	0.0
7753.502	0.019	0.033	0.018	74.1	-0.7	-59.2	0.8	-0.8	-0.2
7754.496	0.019	0.033	0.268	-0.6	-2.4	16.7	-0.4	1.9	2.5
7755.515	0.019	0.033	0.525	-57.0	-1.0	77.9	-0.2	--	--
7772.419	0.019	0.033	0.787	25.1	0.5	--	--	--	--

Notes to TABLE 2

1. An asterisk beside a residual indicates that the residual is larger than three times the root-mean-square value for observations of the same weight as the one indicated; such observations were rejected from the final orbital solution.
2. Superscripts indicate the number of individual observations used to form the nightly means tabulated here.

signed weight 20 (10 for Kitt Peak 2.1 m and Mt. Wilson 2.5 m data), non-CHARA speckle data 5, ''large telescope'' visual data 1, and ''small telescope'' visual data 0.5. Visual ''data'' that are actually means of several observations were assigned weights consisting of the above values multiplied in each case by the square root of the number of observations averaged. Speckle observations of poorer quality are given half the weight they would otherwise have received. Initially, separate solutions were obtained from the position angles and separations, and these gave standard errors of observations of unit weight $\sigma_\theta=3\overset{\circ}{.}2$ and $\sigma_\rho=0\overset{''}{.}10$. They were followed by a two-dimensional solution from both quantities simultaneously in which, to two significant figures, the values of σ_θ and σ_ρ remained unchanged, an indication of the excellent agreement between the elements in common from the separate solutions.

Next, triple-system spectroscopic solutions were obtained with the visually-determined period imposed upon them. Separate triple-lined solutions were first obtained from the data set out in Tables 1, 2, and 3, the residuals from which were used to study zero points and obtain relative weights. Both the McDonald/Kitt Peak and DAO data have zero points tied to the system of Scarfe *et al.* (1990), which was shown by those authors to agree with that of CORAVEL for objects of spectral type similar to that of HD 202908. As might be expected, the velocities from all three sets gave closely similar systemic velocities. However, the variance of the DAO data was about three times, and that of the CORAVEL data about five times, that of the McDonald/Kitt Peak data. The former two data sets were therefore accorded group weights of 1/3 and 1/5, respectively, and a combined solution run for all three sets together. The orbital elements from this solution were then used to determine the zero-point adjustment and relative weight of the Russian data (Table 4), since the latter's phase coverage in the long-period orbit was insufficient to yield an independent solution. These residuals indicated that an adjustment of only $+0.5$ km s^{-1} was required to bring those data onto the same system, with group weight 1/10. A final combined solution was run for all four data sets together, and that solution gave a standard error of unit weight $\sigma_V = 0.56$ km s^{-1}.

The differences between the values of the elements common to both the visual-binary solution and spectroscopic triple-system one, that were obtained from those solutions, were all less than twice their respective uncertainties. Therefore, the two kinds of data were then combined in a simul-

TABLE 3. DAO radial velocities.

Hel. J.D. −2440000	Mask code	Light-time correction (days)	Long-period phase	Short-period phase	V_{Aa} km s^{-1}	O-C$_{Aa}$ km s^{-1}	V_{Ab} km s^{-1}	O-C$_{Ab}$ km s^{-1}	V_B km s^{-1}	O-C$_B$ km s^{-1}
4618.616	F1	-0.018	0.923	0.596	-48.5	-0.1	63.7	-0.1	5.6	-0.7
4720.970	F1	-0.018	0.927	0.404	-48.1	-0.3	63.4	0.1	6.5	0.3
4813.911	K1	-0.018	0.930	0.838	41.1	0.0	-30.5	-0.1	2.8	-3.3*
4842.834	F1	-0.018	0.931	0.130	51.5	0.3	--	--	4.8	-1.2
4951.595	K1	-0.018	0.935	0.553	-55.6	0.5	69.3	-3.1*	5.7	-0.1
5217.751	K2	-0.018	0.944	0.662	-26.4	1.9	42.8	-0.7	5.8	0.5
5288.626	K2	-0.018	0.947	0.532	-58.0	0.0	75.4	0.3	6.6	1.5
5349.580	F1	-0.018	0.949	0.901	58.8	-2.0	-51.5	-1.4	3.9	-1.1
5567.826	K2	-0.017	0.957	0.930	67.4	0.4	-56.3	-0.2	4.5	0.2
5609.768	F1	-0.017	0.958	0.505	-58.8	0.0	78.4	1.6	4.0	-0.1
5625.701	F1	-0.017	0.959	0.522	-58.0	0.2	76.3	0.0	5.1	1.1
5887.934	K2	-0.016	0.968	0.642	-34.6	-0.6	50.6	-1.3	1.9	-0.8
5934.844	K3	-0.016	0.969	0.469	-58.6	-1.8	74.1	-2.1	3.9	1.5
5936.804	K3	-0.016	0.969	0.964	71.3	-1.1	-62.1	-2.1	1.5	-0.9
5952.802	K3	-0.016	0.970	0.997	75.4	1.4	-61.2	0.5	1.8	-0.4
6045.564	K3	-0.015	0.973	0.386	-40.4	0.9	60.6	-0.1	6.6	5.1*
6069.577	K3	-0.015	0.974	0.441	-51.8	1.1	73.8	0.6	4.9	3.7*
6273.924	K4	-0.013	0.981	0.964	74.8	0.7	-57.6	0.9	-1.4	-0.1
6299.878	K4	-0.013	0.982	0.508	-55.9	0.3	79.5	0.1	0.3	2.1
6345.768	K4	-0.012	0.984	0.079	67.7	-0.3	-51.7	-0.8	-1.7	1.0
6378.672	K4	-0.012	0.985	0.375	-37.1	-1.0	59.8	0.2	-3.3	0.1
6565.988	K4	-0.008	0.991	0.604	-39.8	-0.3	68.7	0.2	-7.4	1.8
6616.927	K4	-0.007	0.993	0.448	-50.2	-1.8	80.1	0.2	-9.4	2.1
6641.906	K4	--	0.994	--	--	--	--	--	-12.7	0.0
6669.828	K4	-0.006	0.995	0.786	30.3	0.3	--	--	--	--
6707.796	K4	-0.005	0.996	0.359	-23.8	1.7	58.8	-1.0	--	--
6732.680	K4	-0.004	0.997	0.633	--	--	63.8	0.3	--	--
6763.628	K4	-0.003	0.998	0.436	-42.5	1.0	83.5	2.5	-19.5	-1.1
6902.999	K4	0.002	0.003	0.576	--	--	78.1	-1.2	--	--
6911.001	K4	0.003	0.003	0.593	--	--	76.6	1.2	--	--
6984.933	K4	--	0.006	--	--	--	--	--	-16.7	-0.9
6987.849	K4	0.005	0.006	0.969	82.0	1.3	-53.9	-1.3	-14.4	1.3
7017.866	K4	0.006	0.007	0.537	-49.1	-0.1	83.6	0.4	-14.1	0.4
7019.826	K4	0.006	0.007	0.031	80.3	0.3	-53.5	-0.5	-12.2	2.2
7055.764	K4	0.008	0.008	0.093	69.2	-0.5	-44.0	-0.7	-10.9	2.1
7072.749	K4	0.008	0.009	0.375	--	--	64.7	1.2	--	--
7138.589	K4	0.010	0.011	0.976	80.4	1.6	-56.6	-1.1	-11.2	-1.0
7146.578	K4	0.010	0.012	0.990	78.2	-1.1	-58.2	-2.0	-8.0	1.9
7260.026	K4	0.012	0.016	0.594	-42.8	0.2	71.5	1.4	-3.4	3.6*
7264.0193	K4	0.0123	0.016	0.601	-41.2	0.2	68.4	0.0	-5.2	1.7
7277.9935	F2	0.0126	0.016	0.124	58.2	-0.4	-37.2	0.2	-4.6	2.0
7324.9371	K4	0.0134	0.018	0.960	75.2	-0.4	-56.4	-0.2	-3.9	1.8
7328.9556	K4	0.0135	0.018	0.974	77.2	0.6	-57.0	0.4	-4.9	0.7
7346.9288	K4	0.0138	0.019	0.505	-53.6	1.1	81.4	0.5	-2.1	3.2*
7384.8515	K4	0.0144	0.020	0.067	70.9	-0.2	-52.0	0.4	-3.6	1.0
7422.7420	K4	0.0150	0.021	0.621	-37.3	0.1	61.2	-0.4	-3.6	0.4
7443.6176	K4	0.0153	0.022	0.884	61.3	1.2	-42.2	-0.6	-3.8	0.0
7499.6096	K4	0.0161	0.024	0.002	75.0	-1.3	-60.4	-1.0	-3.3	-0.3
7628.0051	F2	0.0177	0.028	0.375	-37.7	-0.9	59.2	0.4	-1.2	0.4
7721.9081	K4	--	0.032	--	--	--	--	--	-0.5	0.3
7725.8816	K4	0.0188	0.032	0.053	71.6	0.0	-55.5	0.8	1.8	2.6
7745.8559	K4	0.0190	0.033	0.090	64.6	-0.3	-49.7	-0.2	0.2	0.9
7800.7849	K4	0.0195	0.034	0.939	71.1	0.5	-57.6	-1.8	0.2	0.5
7878.5639	F2	0.0202	0.037	0.550	-54.4	-0.4	74.3	-0.9	0.4	0.2
8080.9389	K4	0.0218	0.044	0.577	-51.0	-0.7	70.2	-0.1	2.5	1.2
8109.8546	K4	0.0221	0.045	0.868	53.8	0.8	-39.0	-0.2	1.2	-0.2
8110.8540	F2	0.0221	0.045	0.120	55.3	-1.1	-43.0	-0.7	1.3	-0.1
8116.8228	F2	0.0221	0.045	0.625	-38.7	0.0	57.2	-0.8	3.6	2.1
8165.7251	K4	0.0224	0.047	0.955	72.4	0.6	-59.2	-0.4	--	--
8193.6192	K4	0.0226	0.048	0.988	74.2	0.1	-61.3	0.0	3.2	1.4
8403.9522	F2	0.0239	0.055	0.021	73.5	0.2	-60.5	0.7	4.6	2.1
8455.8800	F2	0.0242	0.057	0.114	57.2	-0.2	-44.6	-0.1	3.6	0.9
8465.8502	F2	0.0242	0.058	0.628	-38.9	-0.6	57.0	0.6	3.7	1.0
8520.7283	K4	0.0245	0.060	0.465	-57.6	-1.0	74.9	-0.7	3.5	0.7
8606.5721	F2	0.0249	0.063	0.109	59.1	0.6	-46.7	-0.7	2.4	-0.7
8780.9546	K4	0.0256	0.069	0.078	66.4	0.9	-54.8	-1.0	4.2	0.7
8800.9349	K4	0.0257	0.069	0.116	56.3	-0.2	-44.9	-0.5	1.8	-1.7
8807.9017	F2	0.0258	0.070	0.872	55.0	1.4	-41.5	-0.2	3.6	0.1
8816.9001	K4	0.0258	0.070	0.141	49.0	0.1	-34.8	1.5	4.1	0.5
8819.8647	K4	0.0258	0.070	0.889	59.6	1.4	-47.6	-1.4	2.4	-1.2
8822.8536	F2	0.0258	0.070	0.642	-34.3	-0.2	51.3	0.0	3.5	-0.1
8833.8702	K4	0.0259	0.070	0.420	-50.3	0.0	67.3	-1.0	3.3	-0.3
8861.8203	K4	0.0260	0.071	0.467	-57.6	-0.4	74.5	-1.0	6.3	2.6
9174.9085	K4	0.0270	0.082	0.409	-48.6	-0.3	65.8	0.2	5.8	1.6
9182.8833	F2	0.0270	0.083	0.420	-50.0	0.6	70.1	2.1	3.0	-1.2
9228.7575	F2	0.0272	0.084	0.987	72.9	0.0	-58.9	3.5*	3.9	-0.4
9242.7576	K4	0.0272	0.085	0.517	-59.0	-0.4	77.3	0.9	3.9	-0.4
9244.7376	F2	0.0272	0.085	0.016	72.5	-0.3	-61.5	0.7	4.9	0.6
9250.7185	F2	0.0272	0.085	0.524	-57.6	0.7	76.5	0.5	5.0	0.7
9262.6980	K4	0.0273	0.085	0.545	-56.6	-0.1	73.7	-0.5	4.0	-0.4
9270.7172	K4	0.0273	0.086	0.566	-54.0	-0.5	71.0	0.1	5.0	0.6
9285.6383	K4	0.0273	0.086	0.329	-25.4	-1.3	40.5	0.6	4.8	0.4
9295.6345	F2	0.0274	0.087	0.849	46.3	0.5	-34.0	-0.2	2.2	-2.2
9519.9107	F2	0.0279	0.094	0.398	-46.4	-0.6	61.3	-1.3	6.8	2.1
9541.9079	K4	0.0280	0.095	0.944	69.1	0.0	-57.3	1.4	5.4	0.7
9547.9026	F2	0.0280	0.095	0.456	-56.2	0.3	73.7	-0.1	3.5	-1.2
9557.8996	K4	0.0280	0.096	0.977	72.9	0.6	-62.5	-0.4	2.7	-2.1
9601.8194	K4	0.0281	0.097	0.050	67.9	-1.6	-61.6	-2.4	4.8	0.0
9628.7268	K4	0.0281	0.098	0.835	40.4	-0.2	-27.5	1.3	6.8	2.0
9633.6992	F2	0.0282	0.098	0.089	63.5	0.8	-52.8	-0.7	4.6	-0.2
9663.6135	K4	0.0282	0.099	0.631	-37.4	0.8	54.1	-0.3	4.9	0.0
9676.5746	K4	0.0282	0.100	0.899	59.1	-1.2	-50.3	-0.7	4.5	-0.4
9691.5793	K4	0.0283	0.100	0.682	-21.9	-1.4	37.6	1.9	5.3	0.4

Notes to TABLE 3

1. An asterisk beside a residual indicates that the residual is larger than three times the root-mean-square value for observations of the same weight as the one indicated; such observations were rejected from the final orbital solution.
2. The following amounts (in km s^{-1}) have been added to the raw velocities obtained with each mask to give the results in this table, which are on the system of Scarfe *et al.* (1990): F1, -0.6: F2, -0.8; K1, 0.8; K2, 0.6: K3, 0.0: K4, 0.4.

taneous three-dimensional solution, using σ_θ=3°.2, σ_ρ=0″.10, and $\sigma_V = 0.56$ km s^{-1}. The elements from that solution are presented in Table 7 and yield the light-time corrections (to the center of mass of the triple system) and velocity residuals in Tables 1 to 4, and the visual and speckle residuals in Tables 5 and 6, respectively. The short-period orbit's eccentricity, although small, is believed to be real since it is just

TABLE 4. Crimea radial velocities.

Hel. J.D. −2440000	Light-time correction (days)	Long-period phase	Short-period phase	V_{Aa} km s^{-1}	O-C$_{Aa}$ km s^{-1}	V_{Ab} km s^{-1}	O-C$_{Ab}$ km s^{-1}	V_B km s^{-1}	O-C$_B$ km s^{-1}
6630.494	-0.007	0.994	0.869	58.6	-0.7	--	--	--	--
6636.488	-0.007	0.994	0.380	-32.2	1.2	61.8	-3.2	--	--
6637.505	-0.007	0.994	0.636	--	--	57.8[2]	-2.6	--	--
6638.445	-0.007	0.994	0.873	58.7	-2.2	--	--	--	--
6640.501	-0.007	0.994	0.392	-40.6	-4.0	66.9	-1.5	-15.8	-3.1
6641.474	-0.007	0.994	0.637	-28.5	0.2	59.8	-0.4	-15.4	-2.7
6642.498	-0.007	0.994	0.895	65.4	-1.6	--	--	--	--
6643.460	-0.007	0.994	0.138	57.4	0.2	-28.4	2.0	-11.6	1.2
6644.396	-0.007	0.994	0.374	--	--	63.3	0.0	--	--
6644.547	-0.007	0.994	0.412	-41.3	0.0	72.7	-1.0	-16.3	-3.4
6645.470	-0.006	0.994	0.644	-22.4	3.8	--	--	--	--
6646.345	-0.006	0.994	0.865	55.4	-3.2	-32.8	-1.1	--	--
6646.559	-0.006	0.994	0.919	74.3	1.8	--	--	--	--
6647.359	-0.006	0.994	0.121	62.8	0.4	-33.4	2.3	--	--
6647.491	-0.006	0.994	0.154	52.8	0.9	-24.4	0.2	-14.3	-1.3
6730.283	-0.004	0.997	0.029	78.7	-2.7	-50.1	1.9	--	--
7003.474	0.006	0.007	0.909	71.1	-0.1	-45.6	-2.5	--	--
7023.403	0.006	0.007	0.933	74.7	-1.0	-48.4	0.2	--	--
8078.488	0.022	0.044	0.959	72.8	0.4	-59.6	-0.5	0.7	-0.6
8079.489	0.022	0.044	0.211	24.0	-0.2	--	--	--	--
8080.483	0.022	0.044	0.462	-53.9	1.7	76.4	0.4	3.9	2.6
8081.504	0.022	0.044	0.719	--	--	19.8	-2.1	--	--
8082.473	0.022	0.044	0.964	74.0	1.2	-57.0	2.6	3.6	2.3
8113.426	0.022	0.045	0.768	17.0	1.1	--	--	--	--
8843.395	0.026	0.071	0.822	37.9	1.6	-22.7	0.4	3.6	0.0
8844.410	0.026	0.071	0.078	64.9	-0.7	-49.6	4.4	3.7	0.1
8845.389	0.026	0.071	0.324	-23.8	-1.6	41.5	2.9	3.9	0.3
8846.373	0.026	0.071	0.573	-49.5	2.6	68.3	-1.8	3.8	0.2
8853.352	0.026	0.071	0.332	-26.1	-1.0	46.6	5.0	4.9	1.3
8854.391	0.026	0.071	0.594	-45.8	1.8	64.9	-0.5	4.5	0.9

Notes to TABLE 4

1. The superscript [2] on the observation of J.D. 2446637 indicates that two observations were averaged to give the tabulated velocity.
2. A zero-point adjustment of +0.5 km s^{-1} has been added to the original velocities to obtain the data in this table.

over four times its own error and since it, together with the corresponding ω, is consistent with the values of those quantities obtained from the separate spectroscopic solutions of the McDonald/Kitt Peak, DAO, and CORAVEL data sets described in the previous paragraph. The velocity curves are shown in Figs. 2 and 3, and the ellipse fitted to the visual and speckle data in Fig. 4. As in the case of the visual-binary solution, the values of σ_θ, σ_ρ, and σ_V remained unchanged to two significant figures, an indication that the elements accurately represent all the data. Indeed the elements in common between the three-dimensional solution and both the visual and spectroscopic solutions that preceded it show excellent agreement. There is also a satisfying degree of agreement between our solution and the recent visual one of Heintz (1994). The values of the angular major semiaxis and eccentricity agree almost exactly, and the small differences between our values of the other elements and his results can probably be attributed to different choices of data used and different weighting schemes, and not to the incorporation of radial velocities into our solution.

As a matter of interest we obtained two additional solutions. The first forced circularity on the short-period orbit; the application of Bassett's (1978) second test (Lucy 1989) provided additional support for the significance of its eccentricity. The second did not make use of light-time corrections, and a standard variance-ratio test indicated that their use had led to a reduction of the sum of the weighted squares of the velocity residuals of the close pair which was significant at the 5% level (the reduction was actually 19%). This differs from the case of HR 6469 (Scarfe *et al.* 1994), in which the reduction was smaller and of less statistical significance.

We note that the number of rejected interferometric measurements might be viewed as unusually high, considering that HD 202908 does not present a particularly difficult case for speckle interferometry. We briefly comment on some of

TABLE 5. Visual data.

Besselian Year	Phase	Position Angle (deg)	O−C$_\theta$ (deg)	Separation (arcsec)	O−C$_\rho$ (arcsec)	Weight	Telescope Size Code
1876.09	0.586	252.3	-3.2	1.16	0.21	1.0	S
1878.60	0.618	254.4	-0.8	0.95	0.02	0.5	S
1883.67	0.683	255.4	0.9	1.17	0.29	0.7	S
1885.60	0.707	252.1	-2.2	1.22	0.37	1.0*	L
1887.795	0.735	251.3	-2.6	0.68	-0.13	1.7	L
1891.52	0.783	254.6	1.4	0.75	0.01	1.7	L
1894.74	0.824	250.8	-1.7	0.56	-0.09	2.6	L
1895.70	0.836	246.9	-5.3	0.63	0.00	1.4	L
1898.74	0.875	250.6	-0.6	0.63	0.11	1.0	S
1899.63	0.886	249.7	-1.1	0.69	0.20	1.0	L
1899.84	0.889	255.5	4.7	0.69	0.21	1.4	L
1910.71	0.027	244.4*	-43.8	0.90	0.84	0.7*	S
1914.50	0.076	264.2	-1.3	0.35	0.07	1.7	L
1915.54	0.089	267.8	3.5	0.30	-0.03	1.4	L
1916.62	0.103	259.0	-4.4	0.38	0.00	1.7	L
1917.698	0.116	263.1	0.5	0.35	-0.07	1.4	L
1918.636	0.128	261.4	-0.7	0.38	-0.08	2.0	L
1920.63	0.154	262.4	1.2	0.51	-0.02	1.4	L
1920.90	0.157	261.8	0.7	0.78	0.24	0.7	S
1921.077	0.159	261.9	0.8	0.49	-0.06	2.0	L
1921.84	0.169	253.1	-7.7	0.69	0.12	1.0	S
1923.69	0.193	259.0	-1.2	0.64	0.01	1.4	L
1924.097	0.198	260.5	0.4	0.56	-0.08	2.0	L
1924.55	0.204	261.7	1.7	0.72	0.07	1.0	L
1924.76	0.206	259.2	-0.7	0.66	0.00	1.4	L
1924.78	0.207	258.9	-1.0	0.76	0.10	1.0	L
1926.75	0.232	258.4	-1.1	0.68	-0.02	1.4	L
1927.68	0.244	256.2	-3.1	0.75	0.02	1.4	L
1933.61	0.319	260.5	2.3	0.73	-0.11	0.7	S
1933.70	0.320	255.8	-2.4	0.74	-0.10	1.4	L
1933.73	0.321	258.6	0.4	0.86	0.02	2.0	L
1933.78	0.321	258.3	0.1	0.95	0.11	0.5	S
1934.60	0.332	256.1	-2.0	0.77	-0.08	1.0	S
1934.73	0.333	252.4	-5.6	0.95	0.09	1.2	S
1936.83	0.360	255.6	-2.1	0.85	-0.03	1.0	L
1938.83	0.386	254.3	-3.2	0.94	0.03	1.2	S
1939.52	0.394	255.7	-1.7	0.96	0.05	1.0	S
1939.67	0.396	254.2	-3.2	0.86	-0.05	1.4	L
1939.70	0.397	256.0	-1.3	0.97	0.06	1.0	S
1939.86	0.399	252.0	-5.3	0.97	0.05	1.0	S
1940.83	0.411	254.4	-2.8	1.01	0.09	1.5	S
1941.84	0.424	255.0	-2.1	0.94	0.01	1.2	S
1942.54	0.433	257.9	0.9	1.07	0.13	0.9	S
1942.75	0.436	254.8	-2.2	0.98	0.04	1.4	S
1945.67	0.473	259.5	2.9	1.01	0.06	1.0	L
1945.79	0.474	252.6	-4.0	1.02	0.07	1.3	S
1945.80	0.474	255.9	-0.7	0.96	0.01	2.0	L
1947.79	0.500	254.7	-1.6	0.96	0.00	0.9	S
1949.75	0.525	254.2	-1.9	1.12	0.16	0.5	S
1949.82	0.526	257.3	1.2	0.88	-0.08	2.0	L
1950.59	0.535	256.7	0.7	0.93	-0.03	0.9	S
1950.76	0.538	255.0	-1.0	0.67	-0.29	1.0	L
1950.78	0.538	251.0	-5.0	1.11	0.15	1.4	S
1951.71	0.550	256.8	0.9	0.83	-0.12	1.4	L
1951.78	0.551	253.1	-2.8	1.10	0.14	1.3	S
1952.53	0.560	256.5	0.7	0.93	-0.02	2.2	L
1952.85	0.564	255.6	-0.1	0.91	-0.04	1.0	S
1952.86	0.564	250.6	-5.1	1.18	0.23	1.4	S
1953.62	0.574	256.8	1.1	0.76	-0.19	1.7	L
1953.82	0.577	251.2	-4.4	1.14	0.19	1.5	S
1954.71	0.588	262.9	7.4	0.64	-0.30	1.4*	L
1954.79	0.589	251.7	-3.8	1.08	0.14	1.4	S
1955.66	0.600	255.6	0.2	0.89	-0.05	1.0	S
1955.68	0.600	252.0	-3.4	0.59	-0.35	1.0*	L
1955.73	0.601	255.5	0.1	0.91	-0.03	1.0	S
1955.74	0.601	251.0	-4.4	1.02	0.08	1.3	S
1955.78	0.602	254.7	-0.7	0.97	0.03	1.4	L
1956.64	0.613	256.4	1.1	0.89	-0.04	0.7	S
1956.79	0.614	251.7	-3.6	0.99	0.06	1.3	S
1957.48	0.623	254.6	-0.6	0.91	-0.02	2.0	L
1957.62	0.625	256.3	1.1	0.91	-0.02	0.9	S
1957.64	0.625	254.6	-0.5	0.68	-0.24	1.4	L
1957.73	0.626	252.9	-2.2	0.88	-0.04	1.7	L
1957.74	0.627	254.1	-1.0	0.82	-0.10	1.0	S
1957.80	0.627	251.8	-3.3	1.01	0.09	1.4	S
1958.59	0.637	255.8	0.8	0.86	-0.06	2.0	L
1958.61	0.638	255.8	0.8	0.92	0.00	1.7	L
1959.55	0.650	257.0	2.1	0.95	0.04	1.1	S
1959.66	0.651	256.4	1.5	0.76	-0.15	1.0	L
1960.67	0.664	257.1	2.3	0.89	-0.01	0.9	S
1960.689	0.664	252.6	-2.1	0.91	0.01	1.4	L
1960.765	0.665	255.3	0.6	0.95	0.06	1.0	L
1961.52	0.675	256.9	2.3	0.83	-0.06	2.0	L
1961.63	0.676	256.4	1.8	0.93	0.05	1.0	S
1961.765	0.678	258.3	3.7	0.89	0.01	1.7	L
1961.81	0.678	254.6	0.0	0.85	-0.03	1.0	S
1961.91	0.680	254.6	0.0	0.77	-0.11	2.0	L
1963.689	0.702	256.6	2.3	0.89	0.03	2.0	L
1963.853	0.704	251.8	-2.5	0.75	-0.10	0.5	S
1965.33	0.723	253.4	-0.7	0.82	-0.01	1.0	S
1965.530	0.726	252.5	-1.5	0.85	0.02	2.0	L
1965.66	0.727	256.5	2.5	0.76	-0.06	1.4	L
1965.74	0.729	252.6	-1.4	0.89	0.07	1.0	S
1966.513	0.738	257.0	3.1	0.82	0.01	1.7	L
1966.584	0.739	250.2	-3.7	0.85	0.04	1.0	L
1966.63	0.740	250.6	-3.3	0.71	-0.10	1.7	L
1966.648	0.740	249.6	-4.2	0.70	-0.11	1.7	L
1967.690	0.753	252.1	-1.6	0.65	-0.14	1.0	L
1967.739	0.754	250.6	-3.1	0.62	-0.17	1.0	L
1968.709	0.766	254.8	1.3	0.81	0.04	2.0	L
1968.92	0.769	251.0	-2.4	0.75	-0.01	1.0	S
1969.34	0.774	253.9	0.5	0.74	-0.01	1.0	S
1970.828	0.793	255.9	2.8	0.80	0.08	2.0	L
1971.779	0.805	255.9	3.0	0.73	0.04	1.7	L
1972.64	0.816	254.0	1.4	0.64	-0.03	2.0	L
1972.665	0.817	250.0	-2.6	0.67	0.00	1.0	L
1972.722	0.817	253.2	0.6	0.70	0.03	2.0	L
1973.597	0.829	250.7	-1.7	0.70	0.06	2.0	L
1973.741	0.830	254.0	1.6	0.62	-0.02	2.0	L
1974.568	0.841	251.7	-0.4	0.48	-0.13	1.7	L
1974.736	0.843	249.9	-2.2	0.65	0.04	1.4	L
1974.821	0.844	253.8	1.7	0.50	-0.10	2.0	L
1975.616	0.854	253.5	1.7	0.54	-0.04	2.0	L
1976.582	0.867	252.9	1.4	0.43	-0.12	1.7	L
1976.819	0.870	252.6	1.2	0.42	-0.12	2.0	L
1977.527	0.879	250.3	-0.8	0.47	-0.04	1.0	L
1977.69	0.881	249.2	-1.8	0.47	-0.03	1.7	L
1978.444	0.890	255.8	5.1	0.39	-0.08	2.0	L
1979.794	0.908	254.4	4.5	0.34	-0.07	2.0	L
1981.507	0.929	251.6	3.0	0.32	-0.01	2.4	L
1988.84	0.023	270.8	-30.7	0.15	0.11	2.0*	L
1992.80	0.073	263.1	-2.7	0.17	-0.10	1.7	L

Notes to TABLE 5

1. An asterisk beside the weight of an observation indicates that at least one of the residuals in θ and ρ is larger than three times the root-mean-square value for observations of the same weight as the one indicated; such observations were rejected from the final orbital solution. The asterisk beside the 1910 position angle measurement indicates that the quadrant has been reversed from that given in the literature.
2. The observations in this table were obtained from the *Washington Double Star Catalogue* database (Worley 1992).

the 12 rejected measures. Five were made with telescopes of 1 m or smaller aperture at epochs where the separation was less than the Rayleigh limit for that telescope. The three rejected CHARA measures have high weights, resulting in more stringent rejection criteria, and one of them was discussed above.

5. $V \sin I$ AND SPECTRAL TYPE

We have determined the projected rotational velocities of the three components from three data sets. In seven CCD spectra the full width at half maximum (FWHM) for each of several relatively unblended lines in the 6430 Å region was measured and averaged for each component. A plot of Gray's (1982, 1984, 1986, 1989) total broadening versus the measured FWHM for 50 stars in common produced a relationship characterized by a polynomial fit. With this calibration the total broadening for each component was determined. To obtain the final $v \sin i$ values, a macroturbulence of 3 km s^{-1} (Soderblom 1982) was assumed. The resulting projected rotational velocities are 11.3±0.5, 10.8±1.0, and 8.0±2.0 km s^{-1} for Aa, Ab, and B, respectively. The errors are estimated from agreement of the multiple measurements and the calibration uncertainties. Such $v \sin i$ values are 2–3 km s^{-1} larger than those estimated by Fekel (1981). Projected rotational velocities were also determined from the CORAVEL observations (Udry 1996) with the method discussed by Benz & Mayor (1981). Assuming $B-V$=0.60 for all three stars, the CORAVEL results are 11.0±0.2, 10.4 ±0.2, and 5.9±0.6 km s^{-1} for Aa, Ab, and B, respectively. A third set was determined from Tokovinin's CORAVEL-type observations. Those results for Aa, Ab, and B are 10.4 ±0.6, 8.6±1.0, and 8.4±1.3 km s^{-1}, respectively. The measured values are in excellent agreement for component Aa, but slightly more scattered for Ab and B. As shown in Fig. 1, the lines from B are the weakest and the central ones of the triplets making it difficult to find unblended lines in the 80 Å wavelength region covered by the CCD observations. Although the errors for each set of rotational velocities were not determined in the same manner, we have nevertheless computed weighted averages for the $v \sin i$ values of each component: 11.0, 10.3, and 6.5 km s^{-1}, for Aa, Ab, and B, respectively.

The spectral types of the three components were determined with the spectrum-addition procedure of Strassmeier

TABLE 6. Speckle-interferometric data.

Besselian Year	Phase	Position Angle (deg)	$O-C_\theta$ (deg)	Separation (arcsec)	$O-C_\rho$ (arcsec)	Telescope Aperture (m)	Weight	Reference
1977.6348	0.880	250.5	-0.6	0.510	0.005	2.1	10.0	M82
1977.7330	0.881	251.3	0.3	0.507	0.006	3.8	20.0	M80
1978.5412	0.892	250.7	0.1	0.480	0.012	3.8	20.0	M80
1978.6177	0.893	251.8	1.2	0.470	0.005	3.8	20.0	M80
1980.4798	0.916	247.9	-1.6	0.394	0.013	3.8	20.0	M83
1981.4628	0.929	248.6	0.0	0.336	0.005	3.8	20.0	M84
1981.4655	0.929	248.7	0.1	0.338	0.008	3.8	20.0	M84
1981.4710	0.929	247.1	-1.5	0.330	0.000	3.8	20.0	M84
1981.7033	0.932	249.6	1.2	0.322	0.004	3.8	20.0	M84
1982.5031	0.942	247.1	-0.2	0.264	-0.009	3.8	20.0	M87
1982.603	0.943	237.6	-9.6	0.210	-0.056	0.6	5.0*	T83
1982.7600	0.945	244.2	-2.7	0.263	0.006	3.8	20.0*	M87
1983.4314	0.954	244.5	-1.1	0.217	0.002	3.8	20.0	M87
1983.7156	0.958	245.6	0.8	0.201	0.005	3.8	20.0	M87
1983.9628	0.961	167.4	-76.7	0.064	-0.115	6.0	5.0*	B85
1984.7040	0.970	241.5	1.1	0.128	0.003	3.8	20.0	M87
1984.780	0.971	240.3	0.4	0.121	0.002	1.0	5.0	T85
1984.8480	0.972	234.3	-5.0	0.119	0.006	6.0	5.0*	B87
1985.4929	0.980	228.8	-0.4	0.126	0.065	3.8	20.0	M87
1985.733	0.983	194.5	-24.4	0.112	0.070	1.0	5.0*	T88
1986.395	0.992	106.2	-0.1	0.046	0.015	1.0	5.0	T88
1986.565	0.994	113.6	20.9	0.041	-0.003	1.0	5.0*	T88
1986.6568	0.995	89.0	0.9	0.046	-0.004	6.0	2.5	B89
1986.7032	0.996	79.9	-6.3	0.057	0.004	6.0	5.0*	B89
1986.8910	0.998	76.4	-3.8	0.061	-0.002	3.8	20.0*	M89
1987.7593	0.009	58.0	1.4	0.056	0.006	3.8	20.0	M89
1988.4162	0.017	350.3	2.1	0.046	0.020	1.0	2.5	I92
1988.5039	0.019	333.8	-0.9	0.054	0.026	1.0	5.0	I92
1988.5174	0.019	336.4	4.7	0.046	0.018	1.0	2.5	I92
1988.6576	0.021	334.3	18.4	0.054	0.021	3.8	10.0*	--
1989.4682	0.031	301.2	19.8	0.050	-0.032	1.0	5.0*	I92
1989.7062	0.034	279.9	1.9	0.098	0.001	3.8	20.0	H92
1990.4326	0.043	318.0	45.7	0.038	-0.104	1.0	5.0*	I92
1990.7546	0.047	271.5	0.7	0.166	0.004	3.8	10.0	H92
1991.9014	0.062	267.5	0.1	0.228	0.002	3.8	20.0	H94
1992.6908	0.072	264.0	-2.0	0.23	-0.038	2.1	2.5	M93
1992.6936	0.072	284.0	18.1	0.29	0.022	2.1	2.5*	M93
1993.9220	0.088	266.9	2.5	0.332	0.005	2.5	10.0	--
1994.7081	0.098	264.1	0.5	0.362	-0.001	3.8	20.0	--
1995.6011	0.109	265.5	2.5	0.399	-0.002	2.5	10.0	--
1995.7594	0.111	263.8	0.9	0.406	-0.002	2.5	10.0	--
1996.5294	0.121	263.5	1.1	0.437	-0.001	2.5	10.0	--

Notes to TABLE 6

1. An asterisk beside the weight of an observation indicates that at least one of the residuals in θ and ρ is larger than three times the root-mean-square value for observations of the same weight as the one indicated; such observations were rejected from the final orbital solution.
2. Codes for references: B85=Balega & Balega 1985, B87=Balega & Balega 1987, B89=Balega & Balega *et al.* 1989; H92=Hartkopf *et al.* 1992, H94=Hartkopf *et al.* 1994; I92=Ismailov 1992, M80=McAlister & Fekel 1980, M82=McAlister & Hendry 1982, M83=McAlister *et al.* 1983, M84 =McAlister *et al.* 1984, M87=McAlister *et al.* 1987, M89=McAlister *et al.* 1989, M93=Miura *et al.* 1993, T83=Tokovinin 1983, T85 =Tokovinin 1985, T88=Tokovinin & Ismailov 1988. Observations without codes are published here for the first time.

TABLE 7. Orbital elements.

	Wide Pair	Close Pair
Period[a] (days)	28685 ± 173	3.9660465 ± 0.0000015
HJD of periastron[a] − 2440000	6812.9 ± 3.0	--
HJD of nodal[b] passage − 2440000	--	6222.5196 ± 0.0007
Velocity amplitude of primary[c] (km s^{-1})	6.13 ± 0.07	66.03 ± 0.06
Velocity amplitude of secondary[c] (km s^{-1})	13.95 ± 0.09	69.69 ± 0.06
Systemic velocity (km s^{-1})	6.24 ± 0.04	variable
Eccentricity	0.8651 ± 0.0008	0.0033 ± 0.0008
Argument of periastron[d]	171°.92 ± 0°.30	271° ± 13°
Inclination	100°.36 ± 0°.16	--
Position angle of node[e]	255°.03 ± 0°.17	--
Angular major semiaxis[f]	0″.5177 ± 0″.0046	--

Notes to TABLE 7

[a]For comparison with the visual and speckle data in Tables 5 and 6, the wide pair's period and date of periastron are, respectively, 78.54±0.47 years and 1987.048±0.008.
[b]Ascending node for component Aa.
[c]In the wide pair the primary is the center of mass of Aa and Ab, and the secondary is B. In the close pair the primary is Aa and the secondary is Ab.
[d]The argument of periastron is for the primary in each case.
[e]The position angle of the node has been adjusted for precession to the equinox of 2000.0.
[f]The angular major semiaxis is that of the relative orbit.

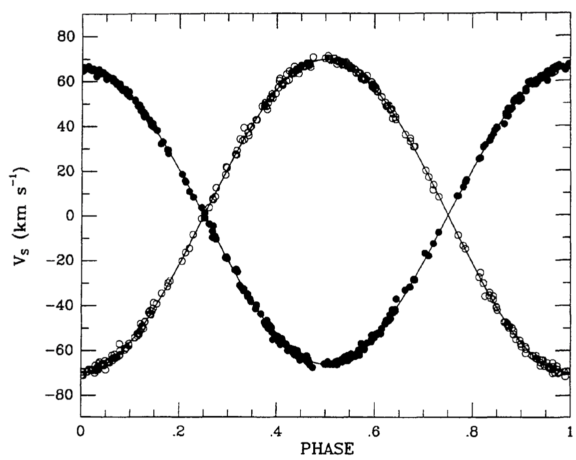

FIG. 2. A comparison of the computed radial-velocity curve for the short-period orbit and the observed velocities. The velocities of Aa are solid circles while those of Ab are open circles.

& Fekel (1990). They identified several luminosity-sensitive and temperature-sensitive line ratios in the 6430 Å region and used them along with the general appearance of the spectrum as spectral-type criteria. A number of late-F and early-G dwarf standards, listed in Strassmeier & Fekel (1990) or Keenan & McNeil (1989), were used for the comparisons. Their spectra were obtained with the same telescope-spectrograph-detector set up as the most recent KPNO observations.

A computer program developed by Huenemoerder & Barden (1984) and Barden (1985) was used to create a three-component comparison spectrum. Three individual standard spectra were summed and shifted in wavelength, while the lines were appropriately broadened. A variety of such triple-lined spectra were compared with those of HD 202908. The best fit, shown in Fig. 1, is with HR 7560 (F8 V) for components Aa and Ab and HR 483 (G1.5 V) for component B. Both reference stars have iron abundances similar to the solar value (Taylor 1994, 1995). A comparison of the spectra

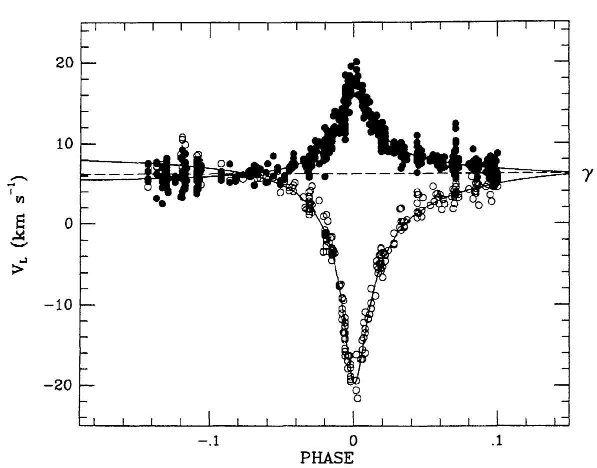

FIG. 3. A comparison of the computed radial-velocity curve for the long-period orbit and the observed velocities. The center-of-mass velocities of A are solid circles while the velocities of B are open circles.

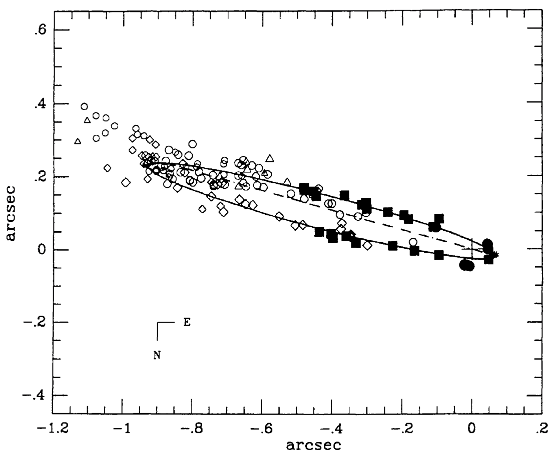

FIG. 4. The computed visual orbit compared with visual and speckle observations. The speckle data are solid symbols with those of CHARA being squares and the rest, circles. Visual data are open symbols. Large-telescope data are plotted as larger symbols than data from small telescopes. The data before the 1909 periastron are triangles, those from the interval 1909 to 1948 (apastron) are diamonds, and those from 1948 until 1992 are circles. The position of the primary star is marked with a plus sign, the line of nodes is shown with alternating dots and dashes, and an asterisk denotes the position of periastron.

of HR 7560 and HR 483 indicates that most of the Fe I lines have nearly identical line strengths. Thus, the continuum intensity ratio Aa:Ab:B=1.0:0.83:0.57 can be converted directly into magnitude differences. Since there is only a slight difference in the $V-R$ colors of HR 7560 and HR 183, the observed magnitude differences of the components of HD 202908 correspond closely to the V-mag differences. The results include $\Delta V_{B-A}=1.26$ mag, $\Delta V_{\mathrm{Ab-Aa}}=0.21$ mag, and $\Delta V_{\mathrm{B-Aa}}=0.61$ mag. The magnitude differences have estimated uncertainties of 0.10 mag.

6. ASTROPHYSICAL PARAMETERS

This section describes the use of the elements presented in Table 7 to determine some fundamental properties of the HD 202908 system. Those properties are summarized in Table 8, with uncertainties obtained by standard error-propagation techniques from those of the elements.

The first section of Table 8 presents results from the short-period orbit alone. They are the standard quantities derivable from a double-lined spectroscopic binary orbit, and need no further description. Since they are derived from radial velocities only, they are necessarily incomplete, but are included because they are useful for deriving the properties of that orbit that appear in the third section and the individual masses of stars Aa and Ab in the second one.

The second section presents results from the long-period orbit, derived from the visual and speckle observations and the radial velocities simultaneously. The orbital parallax is given by

$$\pi_{\mathrm{orb}}=1.086634\times 10^4 a \sin i_L((K_A+K_B)P_L)^{-1} \times(1-e_L^2)^{-1/2}.$$

TABLE 8. Astrophysical results derived from orbital solutions.

1. From the short-period orbit alone	
Mass ratio ($q=\mathcal{M}_{Ab}/\mathcal{M}_{Aa}$)	0.9476 ± 0.0012
$a_{Aa}\sin i_s$ (Gm)	3.6013 ± 0.0034
$a_{Ab}\sin i_s$ (Gm)	3.8006 ± 0.0034
$\mathcal{M}_{Aa}\sin^3 i_s$ ($\mathcal{M}_\odot$)	0.5275 ± 0.0011
$\mathcal{M}_{Ab}\sin^3 i_s$ ($\mathcal{M}_\odot$)	0.4999 ± 0.0010
2. From the long-period orbit alone	
Orbital parallax	0″.01916 ± 0″.00024
Distance (pc)	52.2 ± 0.6
Distance modulus (mag)	3.59 ± 0.03
Mass ratio ($\mathcal{M}_B/\mathcal{M}_A$)	0.440 ± 0.006
Mass fraction ($\mathcal{M}_B/\mathcal{M}_{A+B}$)	0.3053 ± 0.0027
Total mass of system ($\mathcal{M}_\odot$)	3.190 ± 0.063
Masses of stars ($\mathcal{M}_\odot$): Aa	1.138 ± 0.021
Ab	1.078 ± 0.020
B	0.974 ± 0.021
3. Parameters of the short-period orbit derived from the above results	
Inclination	50°.72 ± 0°.46
Major semiaxis (AU)	0.06393 ± 0.00039
(Gm)	9.564 ± 0.059
($R_\odot$)	13.741 ± 0.085
4. Absolute visual magnitudes	
M_{Aa}	4.39 ± 0.10
M_{Ab}	4.60 ± 0.10
M_B	5.00 ± 0.10
5. Angular momenta	
J(close pair) ($\mathcal{M}_\odot AU^2 yr^{-1}$)	1.31 ± 0.04
J(wide pair) ($\mathcal{M}_\odot AU^2 yr^{-1}$)	19.8 ± 0.7
6. Orientation of latter vector is toward	
R.A. (2000)	$15^h\ 5^m.5 \pm 2^m.5$
Dec. (2000)	75°.3 ± 0°.2
Gal. long.	112°.5 ± 0°.2
Gal. lat.	39°.0 ± 0°.2

About half of the uncertainty in that parameter is derived from that of the angular major semiaxis a with the remainder divided roughly equally between those of the period. P_L, and of the velocity amplitudes, K_A and K_B. The eccentricity e_L and inclination i_L, particularly the latter, contribute very little.

The total mass of the system is given by

$$\mathscr{M}=1.03615\times 10^{-7}P_L((K_A+K_B)(1-e_L^2)^{1/2}(\sin i_L)^{-1})^3.$$

We also derive a mass ratio Q and the fraction f of the mass that resides in the visual secondary, which agrees with that of Heintz (1994) within the latter's uncertainty, although the uncertainty of our value is smaller than that of his by a factor just over 10. The mass of each star is readily found from $\mathscr{M}$, Q, and q, the mass ratio in the short-period orbit. About three quarters of the uncertainty in the masses comes from those of the radial-velocity amplitudes.

In the third section of Table 8 we present properties of the orbit of the close pair, derived by combining the total mass of that subsystem with the results in the first section. We note that the minimum angle between the planes of the short- and long-period orbits is 28°.9±0°.5, in agreement with the result of Fekel (1981). The absolute visual magnitudes of the three stars, derived from the spectroscopic luminosity ratios and the orbital parallax, are presented next; their uncertainty is about 0.1 mag in each case. The results are consistent with the stars' spectral types and masses, and confirm their similarity to the sun. Since their radii must also be similar to that of the sun, the separation of the two stars in the close pair is large enough to ensure that (a) tidal distortions of their

TABLE 9. Lithium equivalent widths and abundances.

Component	W_{obs}(Li) (mÅ)	Correction	W_{true}(Li) (mÅ)	Assumed T_e (K)	log ϵ(Li)
Aa	67	2.40	161	6115	3.3
Ab	58	2.90	168	6115	3.4
B	27	4.20	114	5819	2.8

shapes will be small, and (b) eclipses are not to be expected, consistent with the lack of any literature record of such events.

Finally, in Table 8 we present the orbital angular momenta, J_S and J_L, and the direction of the latter vector, determined by the procedure described by Scarfe *et al.* (1994). Precession of the two vectors about their resultant would eventually permit the angle between them to be determined, as discussed by those authors, but that phenomenon is likely to be even slower in the present case, because of the large value of the ratio P_L/P_S.

7. DISCUSSION

As shown by Fekel (1981), all three stars are chromospherically active. Such active stars usually have light variability resulting from star spots rotating in and out of view. Henry *et al.* (1995) reported that their five seasons of photometry of HD 202908 showed no evidence of variability. Thus, the rotational periods of Aa and Ab have not been determined directly. Given the short orbital period, however, those components are almost certainly synchronously rotating. That rotational period and our weighted mean $v \sin i = 11.0 \pm 0.2$ km s^{-1} for Aa result in a minimum radius of 0.86 $R_\odot$. Assuming a radius of 1.16 $R_\odot$ (Gray 1992), produces an inclination of $48° \pm 1°$ compared with an inclination of $50\overset{\circ}{.}7 \pm 0\overset{\circ}{.}5$ for the short-period orbit. Such a result is consistent with the conclusion of Glebocki & Stawikowski (1995) that the rotational and orbital axes of synchronously rotating main-sequence chromospherically active binaries are aligned.

The ages of field stars show statistical correlations with Ca II H and K emission, rotational velocity, and lithium abundances. While the value for a single parameter might be an aberration, consistency of the three diagnostics lent support to Fekel's (1981) age estimate. Here, we briefly reexamine the age of HD 202908 in the context of more recent work on rotational velocities and lithium abundances. Since the short-period pair is presumably tidally locked, it is the cooler B component of the visual binary that is of primary importance. While very young clusters such as the Pleiades and α Per have a wide range of rotational velocities for a given mass, by the age of the Hyades, 0.6 Gyr, there is a significant convergence with G2 dwarfs having $v \sin i \lesssim 7$ km s^{-1} (e.g., Soderblom *et al.* 1993a). Such a result is quite consistent with our weighted $v \sin i$ value for B.

Over the past 15 years lithium abundances have been determined for a wealth of solar-type stars in a variety of clusters. Our results for the three components, Aa, Ab, and B are given in Table 9. Listed are the measured equivalent widths from Fekel (1981), the dilution correction factors, true equivalent widths, assumed effective temperatures from Gray (1992), and log lithium abundances determined with Table 2 of Soderblom *et al.* (1993b). The log abundances have estimated uncertainties of 0.3. The abundances of Aa and Ab are consistent with the maximum values seen in Population I stars, log ϵ(Li)$\sim$3.0–3.3, while the abundance of 2.8 for component B is slightly greater than that found for Hyades stars of similar color. Thus, our updated results remain consistent with the conclusion that HD 202908 has an age similar to the Hyades cluster.

Using the magnitudes in Table 8 and the effective temperatures listed in Table 9, we compared the positions of the individual stars with the $Z=0.020$ theoretical tracks of Schaller *et al.* (1992). All three components of HD 202908 are close to the zero-age main sequence, providing additional support for the young age of the system.

Binaries with short periods usually have circular orbits presumably due to tidal effects (e.g., Zahn 1977) and/or a hydrodynamic mechanism (Tassoul 1987). In triple systems the third star may cause some of the orbital elements of the close pair to vary with time. Changes in the eccentricity have been examined numerically by Mazeh & Shaham (1979) and both analytically and numerically by Söderhjehn (1984). Their results showed that even if the short-period system attained a circular orbit, its eccentricity would be modulated. In support of those conclusions Mazeh (1993) identified three late-type binaries that were expected to have circular orbits but actually had small but significant eccentricities ranging from 0.031 to 0.057. The amplitude of the modulation depends upon several factors including the relative inclination of the orbital planes and arguments of periastron (Mazeh *et al.* 1993), making predictions of expected amplitude variations difficult in individual cases. However, the position of HD 202908 in Söderhjelm's (1981) Fig. 7 suggests that no modulation of the short-period eccentricity is expected because of the very large period ratio of about 7200. From Mazeh & Shaham (1979) we compute a modulation period of 0.47 Gyr for HD 202908, which is roughly the estimated age ($\sim$0.6 Gyr) of the system. Although the very small eccentricity of 0.0033 ± 0.0008 for the short-period orbit may result from the effects of a third body, because the system is believed to be quite young and the convection zones of the stars are relatively shallow, the inner orbit may simply not have had time to circularize completely.

Donnison & Mikulskis (1995) used an analytical method to determine an improved critical condition of stability for triple systems with outer orbits having significant eccentricities. They found that spectroscopic-visual triples, including HD 202908, lie well within the limits of stability and are thus, very stable.

We thank Stephane Udry for communicating some of the CORAVEL results. This research has been supported in part by NASA Grants No. NAG8-1014 and No. NCCW-0085 as well as NSF Grant No. HRD-9550561 to TSU, and in part by grants from the University of Victoria and from the Natural Sciences Research Council of Canada. C.D.S. wishes to express his appreciation for generous allotments of DAO observing time. F.C.F. acknowledges the significant allotments of telescope time at KPNO and the extensive patience and help of Daryl Willmarth and Jeannette Barnes. The speckle interferometry program at Georgia State University has been supported by the National Science Foundation, most recently through Grant No. AST 94-16994, by the Office of the Dean of the College of Arts and Sciences, and by the Chancellor's Initiative Fund, administrated by the Office of the Vice President for Research and Sponsored Programs at GSU. Before this paper could be completed, one of the authors (A.D.) was tragically killed in a highway accident. The remaining authors wish to dedicate this paper to his memory.

REFERENCES

Abt, H. A. 1981, ApJS, 45, 437
Aitken, R. G. 1932, New General Catalog of Double Stars. Vol. 11 (Carnegie Institution, Washington, D. C.), p. 973.
Bagnuolo, Jr., W. G., Mason, B. D., Barry, D. J., Hartkopf, W. I., & McAlister, H. A. 1992, AJ, 103, 1399
Balega, Yu. Yu., & Balega, I. I. 1985, SvAL, 11, 17
Balega, I. I., & Balega, Yu. Yu. 1987, SvAL, 13, 208
Balega, I. I., Balega, Yu. Yu., & Vasyuk, V. A. 1989, Astrofiz. Issled. Izv. Spets. Astrofiz. Obs., 28, 107
Barlow, D. J., Fekel, F. C., & Scarfe, C. D. 1993, PASP, 105, 476
Barden, S. C. 1985, ApJ, 295, 162
Bassett, E. E. 1978, Observatory, 98, 122
Batten, A. H., Fletcher, J. M., & MacCarthy, D. G. 1989, Publ. Dom. Astrophys. Obs., 17, 1
Benz, W., & Mayor, M. 1981, A&A, 93, 235
Burnham, S. W. 1873, MNRAS, 34, 59
Christy, J. W., & Walker, R. L. 1969, PASP, 81, 643
Donnison, J. R., & Mikulskis, D. F. 1995, MNRAS, 272, 1
Duquennoy, A. 1987, A&A, 178, 114
Fekel, F. C. 1981, ApJ, 248, 670
Fekel, F. C. 1991, AJ, 101, 1489
Fekel, F. C. 1992, in Complementary Approaches to Double and Multiple Star Research, IAU Colloquium 135, edited by H. A. McAlister and W. I. Hartkopf (ASP, San Francisco), p. 89.
Fekel, F. C., Bopp, B. W., & Lacy, C. H. 1978, AJ, 83, 1445
Fletcher, J. M., Harris, H. C., McClure, R. D., & Scarfe, C. D. 1982, PASP, 94, 1017
Glebocki, R., & Stawikowski, A. 1995, Acta Astron., 45, 725
Gray, D. F. 1982, ApJ, 258, 201
Gray, D. F. 1984, ApJ, 281, 719
Gray, D. F. 1986, ApJ, 310, 277
Gray, D. F. 1989, ApJ, 347, 1021
Gray, D. F. 1992, The Observation and Analysis of Stellar Photospheres (Cambridge University, New York), p. 431.
Harlan, E. A. 1969, AJ, 74, 916
Hartkopf, W. I., McAlister, H. A., & Franz, O. G. 1989, AJ, 98, 1014
Hartkopf, W. I., McAlister, H. A., & Franz, O. G. 1992, AJ, 101, 810
Hartkopf, W. I., McAlister, H. A., Mason, B. D., Barry, D. J., Turner, N. H., & Fu, H.-H. 1991, AJ, 108, 2299
Hartkopf, W. L., McAlister, H. A., & Mason, B. D. 1995, Third Catalog of Interferometric Measurements of Binary Stars, CHARA Contribution No. 4, (Georgia State University, Atlanta), http://www.chara.gsu.edu/DoubleStars/Catalogues/Speckle/intro.html
Heintz, W. D. 1969, A&A, 2, 169
Heintz, W. D. 1994, AJ, 108, 2338
Henry, G. W., Fekel, F. C., & Hall, D. S. 1995, AJ, 110, 2926
Huenemoerder, D. P., & Barden, S. C. 1984, BAAS, 16, 510
Ismailov, R. M. 1992, A&AS, 96, 375
Keenan, P. C., & McNeil, R. C. 1989, ApJS, 71, 245
Lucy, L. B. 1989, Observatory, 109, 100
Mason, B. D., McAlister, H. A., Hartkopf, W. I., & Bagnuolo, Jr., W. G. 1993, AJ, 105, 220
Mazeh, T. 1993, AJ, 99, 675
Mazeh, T., Krymolowski, Y., & Latham, D. W. 1993, MNRAS, 263, 775
Mazeh, T., & Shaham, J. 1979, A&A, 77, 145
McAlister, H. A., & Fekel, F. C. 1980, ApJS, 43, 327
McAlister, H. A., Hartkopf, W. I., Hendry, E. M., Gaston, B. J., & Fekel, F. C. 1984, ApJS, 51, 251
McAlister, H. A., Hartkopf, W. I., Hutter, D. J., & Franz, O. G. 1987, AJ, 93, 688
McAlister, H. A., Hartkopf, W. I., Sowell, J. R., Dombrowski, E. G., & Franz, O. G. 1989, AJ, 97, 510
McAlister, H. A., & Hendry, E. M. 1982, ApJS, 48, 273
McAlister, H. A., Hendry, E. M., Hartkopf, W. I., Campbell, B. G., & Fekel, F. C. 1983, ApJS, 51, 309
McClure, R. D., Fletcher, J. M., Grundmann, W. A., & Richardson, E. H. 1985, in Stellar Radial Velocities, edited by A. G. D. Philip and D. W. Latham (Davis, Schenectady), p. 49
Miura, N., Ni-ino, M., Baba, N., Iribe, T., & Isobe, S. 1993, Publ. Natl. Astron. Obs. Jpn. 3, 153
Pearce, J. A. 1957, Trans. IAU, 9, 441
Perry, C. L. 1969, AJ, 74, 705
Scarfe, C. D., Barlow, D. J., Fekel, F. C., Rees, R. F., Lyons, R. W., Bolton, C. T., McAlister, H. A., & Hartkopf, W. I. 1994, AJ, 107, 1529
Scarfe, C. D., Batten, A. H., & Fletcher, J. M. 1990, Publ. Dom. Astrophys. Obs., 18, 21
Schaller, G., Schaerer, D., Meynet, G., & Maeder, A. 1992, A&AS, 96, 269
Soderblom, D. R. 1982, ApJ, 263, 239
Soderblom, D. R., Jones, B. F., Balachandran, S., Stauffer, J. R., Duncan, D. K., Fedele, S. B., & Hudon, J. D. 1993b, AJ, 106, 1059
Soderblom, D. R., Stauffer, J. R., Hudon, J. D., & Jones, B. F. 1993a, ApJS, 85, 315
Söderhjelm, S. 1984, A&A, 141, 232
Sterne, T. E. 1941, Proc. U.S. Natl. Acad. Sci., 27, 175
Strassmeier, K. G., & Fekel, F. C. 1990, A&A, 230, 389
Strassmeier, K. G., Hall, D. S., Fekel, F. C., & Scheck, M. 1993, A&AS, 100, 173
Tassoul, J.-L. 1987, ApJ, 322, 856
Taylor, B. J. 1994, PASP, 106, 704
Taylor, B. J. 1995, PASP, 107, 734
Tokovinin, A. A. 1983, SvAL, 9, 293
Tokovinin, A. A. 1985, A&AS, 61, 483
Tokovinin, A. A. 1987, AZh, 64, 196 (SvA, 31, 98)
Tokovinin, A. A., & Ismailov, R. M. 1988, A&AS, 72, 563
Udry, S. 1996, private communication
Wilson, R. E., & Joy, A. H. 1950, ApJ, 111, 221
Worley, C. E. 1992, in Complementary Approaches to Double and Multiple Star Research, IAU Colloquium 135, edited by H. A. McAlister and W. I. Hartkopf (ASP, San Francisco), p. 284
Zahn, J.-P. 1977, A&A, 57, 383